

Supporting Information

Jiu-Hong Yu,^a Zhi-Rui Yuan,^a Jing Xu,^a Jin-Gui Wang,^a Mohammad Azam,^c Tian-Duo Li,^a Ying-Zhou Li,^{*a} and Di Sun^{*b}

^a*School of Chemistry and Chemical Engineering, Qilu University of Technology (Shandong Academy of Sciences), Ji'nan, 250353, P.R. China. E-mail: liyz@qlu.edu.cn*

^b*School of Chemistry and Chemical Engineering, State Key Laboratory of Crystal Materials, Shandong University, Ji'nan, 250100, P.R. China. E-mail: dsun@sdu.edu.cn*

^c*Department of Chemistry, College of Science, King Saud University, P. O. Box 2455, Riyadh 11451, Saudi Arabia.*

Contents

Physical measurements and instrumentation

X-ray crystallography

DFT calculations

Experimental

Figure S1. Stacking diagram of the precursor complex (Ph₃As)AuCl in the unit cell.

Figure S2. Ortep diagram showing the molecular structure of (Ph₃As)₃AuCl.

Figure S3. The two independent molecules of **Au₁₃As₈** in the unit cell and their stacking diagram.

Figure S4. ³¹P{¹H} NMR spectrum of **Au₁₃As₈** in CD₂Cl₂ at room temperature.

Figure S5. Comparative IR spectra of crude and crystalline **Au₁₃As₈**.

Figure S6. ¹H NMR spectra of **Au₁₃As₈** in CD₂Cl₂ at room temperature.

Figure S7. Experimental UV-vis spectra of **Au₁₃As₈**, **Au₁₃Sb₈**, [Au₁₃(PPh₂Me)₈Cl₄]⁺, [Au₁₃(dppp)₄Cl₄]⁺ and [Au₁₃(PR₃)₈Cl₄]⁺ (R = CH₂CH₂CO₂CH₃), and correlations between ligands and absorptions.

Figure S8. Experimental and TD-DFT calculated UV-vis spectra of **Au₁₃As₈**.

Figure S9. Experimental and TD-DFT calculated UV-vis spectra of **Au₁₃Sb₈**.

Figure S10. Photoluminescence spectra for **Au₁₃As₈** (magenta line, λ_{ex} = 460 nm) and **Au₁₃Sb₈** (cyan line, λ_{ex} = 470 nm) in crystalline state at room temperature.

Figure S11. UV-vis monitoring spectra of **Au₁₃As₈** in CH₂Cl₂ stored in dark at 4 °C.

Figure S12. TGA comparison curves of **Au₁₃As₈** and **Au₁₃Sb₈**.

Figure S13. UV-vis spectrum of the recovered **Au₁₃As₈** in DCM after five cycles.

Figure S14. ¹H NMR spectra of the crudes in CD₂Cl₂ for A³ coupling reactions catalyzed by **Au₁₃As₈** and **Au₁₃Sb₈**.

Figure S15. The NMR yields of propargylamine for the A³ coupling reactions catalyzed by **Au₁₃As₈** and **Au₁₃Sb₈**.

Figure S16. Photographs of the crystals of [Au₁₁(PPh₃)₈Cl₂]⁺ and [Au₁₃(dppe)₅Cl₂]³⁺.

Figure S17. UV-vis spectrum of [Au₁₁(PPh₃)₈Cl₂]⁺ in CH₂Cl₂.

Figure S18. ¹H{³¹P} NMR spectrum of [Au₁₁(PPh₃)₈Cl₂]⁺ in CD₂Cl₂.

Figure S19. UV-vis spectrum of [Au₁₃(dppe)₅Cl₂]³⁺ in CH₂Cl₂.

Figure S20. ESI-MS(+) spectrum of [Au₁₃(dppe)₅Cl₂]³⁺ in CH₂Cl₂.

Table S1. Crystallographic Data for **Au₁₃As₈** and (Ph₃As)₃AuCl.

Table S2. Selected bond distances (Å) for crystallographic **Au₁₃As₈** and **Au₁₃Sb₈**.

Table S3. Selected bond distances (Å) for structurally optimized **Au₁₃As₈** and **Au₁₃Sb₈**.

Table S4. Selected orbitals of **Au₁₃As₈** and elemental contribution ratios (%).

Table S5. Selected orbitals of **Au₁₃Sb₈** and elemental contribution ratios (%).

Table S6. Selected excited states, energy, oscillator strength, and the most probable transitions of **Au₁₃As₈** from TD-DFT calculations.

Table S7. Selected excited states, energy, oscillator strength, and the most probable transitions of **Au₁₃Sb₈** from TD-DFT calculations.

Table S8. Cartesian coordinates of optimized **Au₁₃As₈** and **Au₁₃Sb₈**.

Table S9. Natural Population charges for **Au₁₃As₈** and **Au₁₃Sb₈**.

Table S10. Mulliken charges for **Au₁₃As₈** and **Au₁₃Sb₈**.

Table S11. Selected Second Order Perturbation theory analysis of Fock matrix in NBO basis for **Au₁₃As₈**.

Table S12. Selected Second Order Perturbation theory analysis of Fock matrix in NBO basis for **Au₁₃Sb₈**.

Table S13. Selected Wiberg bond indices in the NAO basis for **Au₁₃As₈** and **Au₁₃Sb₈**.

Physical measurements and instrumentation

The UV-Vis spectra were recorded on a Thermo Scientific Evolution 220 UV-visible spectrophotometer. Photoluminescence measurements were carried out in an Edinburgh spectrophotometer (F920S). Mass spectra were recorded on an Agilent 6224 ESI-TOF-MS spectrometer; Sample solutions are infused by a syringe pump at 4 $\mu\text{L}/\text{min}$. Data were acquired using the following settings: ESI capillary voltage was set at 6000 V (+) ion mode and fragmentor at 200 V. The liquid nebulizer was set to 15 psig and the nitrogen drying gas was set to a flow rate of 4 L/min; the data analyses of mass spectra were performed based on the isotope distribution patterns using Agilent MassHunter Workstation Data acquisition software (Version B.05.00); the reported m/z values represent monoisotopic mass of the most abundant peak within the isotope pattern. Infrared spectrum was recorded on a PerkinElmer Spectrum Two in the frequency range of 4000-400 cm^{-1} . TGA measurement was performed on a TGA-Q500 thermogravimetric analyzer at a heating rate of 10 $^{\circ}\text{C}/\text{min}$ under N_2 purge (60 mL/min). ^1H and ^{31}P NMR spectra at room temperature were recorded on a Bruker Advance III 400 MHz spectrometer. ^1H chemical shifts were referenced to the residual proton resonance; ^{31}P chemical shifts were referenced to external 85% aq. H_3PO_4 .

X-ray crystallography

Crystal data of $\text{Au}_{13}\text{As}_8$ and $(\text{Ph}_3\text{As})_3\text{AuCl}$ (side product) were collected on a Rigaku Oxford Diffraction XtaLAB Synergy diffractometer using Cu $K\alpha$ radiation ($\lambda = 1.54178 \text{ \AA}$) at 100 K. A preliminary set of cell constants and an orientation matrix were calculated from reflections harvested from a sampling of reciprocal space. Full data collections were carried out using Cu $K\alpha$ radiation ($\lambda = 1.54184 \text{ \AA}$, PhotonJet-S Cu 50W Microfocus) with exposure time ranging from 0.5 to 2 seconds, frame widths of 1 degree, and a detector distance of approximately 3.2 cm. The intensity data were scaled and corrected for absorption, and final cell constants were calculated from the xyz centroids of strong reflections from the actual data collections after integration. The space groups were determined based on systematic absences and intensity statistics. Absorption correction was applied by using the program CrysAlisPro program.^[1] The structures were solved using the charge-flipping algorithm, as implemented in the *SUPERFLIP* program^[2] and refined by full-matrix least-squares techniques against F_2 using the SHELXL program^[3] through the OLEX2 interface.^[4] Hydrogen atoms were placed in calculated positions and refined isotropically by using a riding model. Appropriate restraints or constraints were applied to the geometry and the atomic displacement parameters of the atoms in the cluster. The structures were examined using the Addsym subroutine of PLATON^[5] to ensure that no additional symmetry could be applied to the models. It should be noted that the possible counter anion PF_6^- was not located, probably due to its severe disorder. Detailed crystallographic data and refinement parameters are given in Table S1.

DFT Calculations

DFT optimizations and TD-DFT UV-vis spectrum calculations of the cationic clusters $[\text{Au}_{13}(\text{AsPh}_3)_8\text{Cl}_4]^+$ (**Au₁₃As₈**) and its stibine analogue $[\text{Au}_{13}(\text{SbPh}_3)_8\text{Cl}_4]^+$ (**Au₁₃Sb₈**) were performed with the Gaussian 16 suite of programs.^[6] The gradient-corrected MPW1PW91 exchange correlation functional based on the generalized gradient approximation (GGA) was used;^[7] the MPW1PW91 functional is expected to be more suitable for the second and third row transition metal systems.^[8] The Los Alamos valence double- ζ with Hay–Wadt ECPs (LanL2DZ) basis set containing relativistic effects was employed for Au and Sb atoms,^[9] and 6-31G(d, p) basis set was used for the remaining atoms.^[10] Crystal structures of **Au₁₃As₈** and **Au₁₃Sb₈** (obtained from literature^[11]) were used for geometry optimizations by spin-restricted calculation; the optimized cartesian coordinates of the corresponding structures are appended in Table S7. A total of 600 singlet states were calculated and the root was set as 1 in the TD-DFT UV-vis spectra calculations. Data for orbital composition analysis with Mulliken partition are from Gaussian 16 calculations and further processed with Multiwfn software.^[12] The most probable transitions were determined based on the oscillator strength values and weights. The optical absorption spectra were convoluted with a Gaussian line shape with a half-width at half-height of 0.25 eV. The optimized structures for **Au₁₃As₈** and **Au₁₃Sb₈** were used for NBO calculations with the NBO 7.0 package embedded in Gaussian 16; the same functional and basis sets were used as those in structural optimization and UV-vis calculations, except that an additional f-type polarization function was added to Au atoms, and an additional d-type polarization function was added to Sb atoms.

Experimental

Materials and methods: Ethanol, dichloromethane (DCM) and hexane were purchased from Sinopharm Chemical Reagent Co., Ltd. $\text{HAuCl}_4 \cdot 3\text{H}_2\text{O}$, KPF_6 , Me_2S , NaBH_4 and all the pnictine ligands were purchased from Aladdin Industrial Corporation (Shanghai, China). Me_2SAuCl and $\text{Au}_{13}\text{Sb}_8$ were prepared according to literatures.^[11,13] All chemicals were used as received without further purification. Details of the physical measurements and instrumentations, X-ray Crystallography, DFT-calculations, catalytic performance of $\text{Au}_{13}\text{As}_8$ towards A^3 coupling reaction, and ligand exchange reactions of $\text{Au}_{13}\text{As}_8$ with phosphines were given in the Supporting Information.

Synthesis of $\text{Au}_{13}\text{As}_8$: Me_2SAuCl (236 mg, 0.80 mmol) and AsPh_3 (246 mg, 0.80 mmol) was first mixed in DCM (20 mL), and the solution was stirred at room temperature for 1 h. The solvent was then pumped off to completely remove the Me_2S and the residual was redissolved in DCM (20 mL) and ethanol (8 mL), followed by addition of KPF_6 (15 mg, 0.08 mmol). Then a freshly prepared solution of NaBH_4 (15.9 mg, 0.42 mmol) in ethanol (6 mL) was dropwise added within *ca.* 2 mins, accompanied by an immediate color change from colorless to dark-red. After further stirring at room temperature for 16 h, the solution was filtered and the solvents were removed. The residual was redissolved in DCM (20 mL), followed by addition of hexane (80 mL) to precipitate the crude product. After washing with DCM/hexane (8 mL/32 mL) three times, the crude was redissolved in DCM/hexane (12 mL/4 mL). After refiltration, slow evaporation of the solution at 4 °C afforded dark-red plate-like crystals of $\text{Au}_{13}\text{As}_8$ within two days (yield: 133 mg; 42% based on $[\text{Au}_{13}(\text{AsPh}_3)_8\text{Cl}_4][\text{PF}_6]$).

Reactions of $\text{Au}_{13}\text{As}_8$ with $\text{Ph}_2\text{P}(\text{CH}_2)_2\text{PPh}_2$ (dppe). $\text{Au}_{13}\text{As}_8$ (54 mg, 10 μmol) was dissolved in DCM (15 mL), followed by addition of dppe (20 mg, 50 μmol). The resulting solution was stirred overnight at room temperature. Hexane (60 mL) was then added and the brown precipitation obtained was redissolved in DCM/ethanol (8 mL/4 mL). After filtration, slow evaporation of the filtrate at room temperature afforded dark-red rod-like crystals of $[\text{Au}_{13}(\text{dppe})_5\text{Cl}_2]^{3+}$ within three days (yield: 38 mg, 76% based on $[\text{Au}_{13}(\text{dppe})_5\text{Cl}_2][\text{PF}_6]_3$).

Reactions of Au₁₃As₈ with PPh₃. Au₁₃As₈ (54 mg, 10 μmol) was dissolved in DCM (15 mL), followed by addition of PPh₃ (50 mg, 0.20 mmol). The resulting solution was stirred overnight at room temperature. Hexane (60 mL) was then added and the brown precipitation obtained was redissolved in DCM/ethanol (9 mL/3 mL). After filtration, slow evaporation of the filtrate at room temperature afforded red plate-like crystals of [Au₁₁(PPh₃)₈Cl₂]⁺ within three days (yield: 18 mg, 41% based on [Au₁₁(PPh₃)₈Cl][PF₆]).

A³ coupling reaction. According to literature procedure,^[14] benzaldehyde (106 mg, 1.0 mmol), piperidine (102 mg, 1.2 mmol) and phenylacetylene (133 mg, 1.3 mmol) were sequentially mixed in a 10 ml of Pyrex tube containing Au₁₃As₈ (0.5 mol%) under ambient conditions. The tube was then capped tightly and the dark-red oil mixture was stirred at room temperature for 12 h. Suitable amount of oil crude was directly drawn into an NMR tube for the ¹H NMR experiments. The Au₁₃As₈ catalysts can be directly recovered/precipitated out by addition of hexane to the mixture.

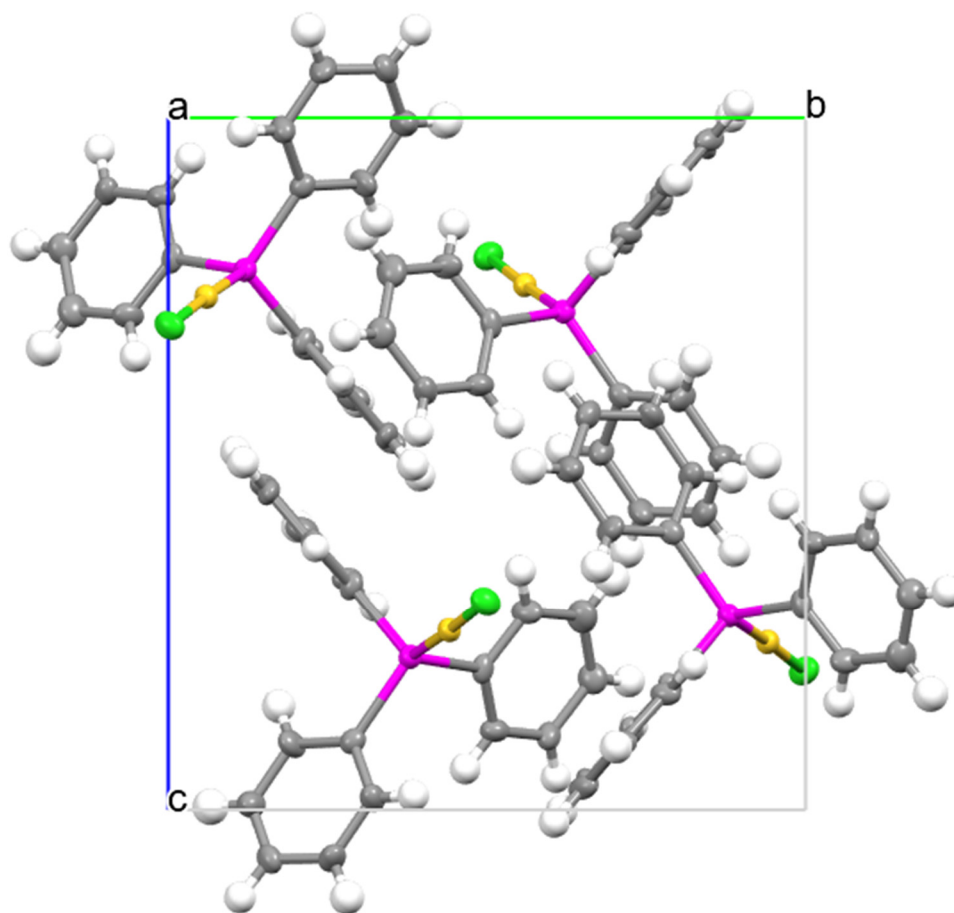


Figure S1. Stacking diagram of the precursor complex (Ph₃As)AuCl in the unit cell.

Note: The same crystal structure was previously reported.^[15] The aim for the repeated measurement was just to verify its identity, and thus no more analysis on this structure was made. Color code: yellow, Au; magenta, As; green, Cl; grey, C.

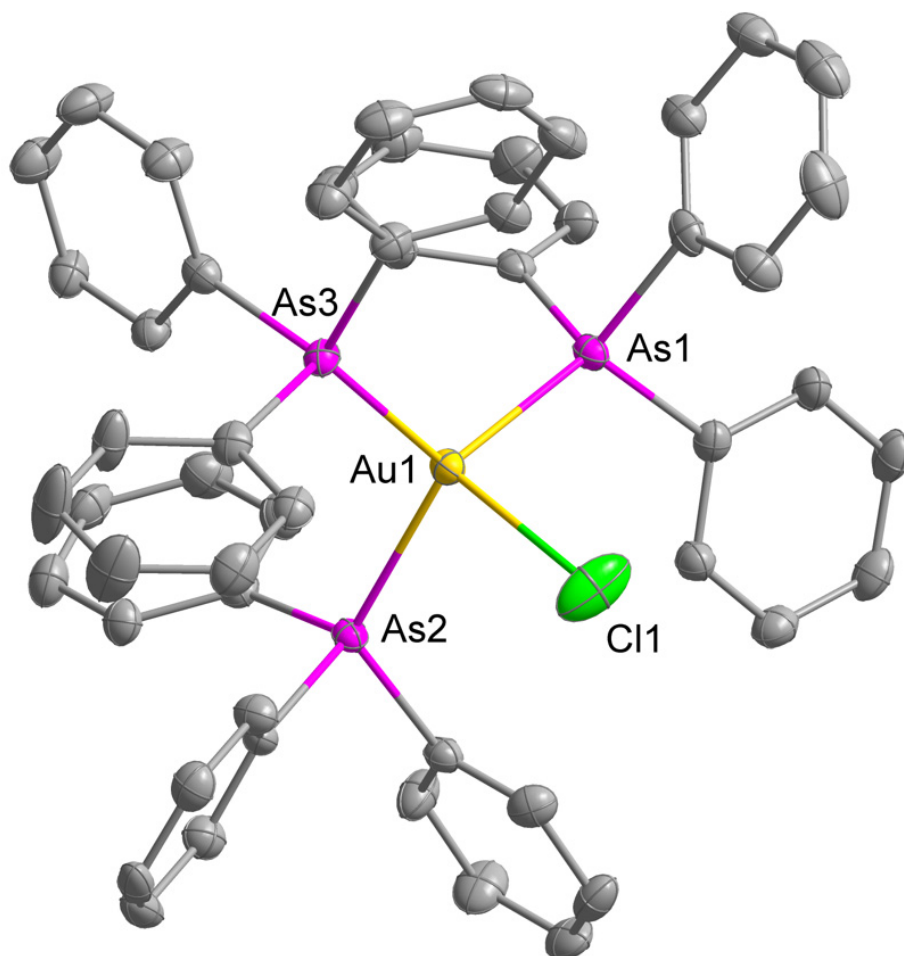


Figure S2. Ortep diagram showing the molecular structure of $(\text{Ph}_3\text{As})_3\text{AuCl}$.

Note: Thermal ellipsoids are drawn at the 50% probability level. Organic hydrogen atoms are omitted for clarity. Selected bond lengths (\AA) and angles ($^\circ$): $\text{Au}(1)\text{-As}(1) = 2.4872(4)$; $\text{Au}(1)\text{-As}(2) = 2.5043(4)$; $\text{Au}(1)\text{-As}(3) = 2.4865(3)$; $\text{Au}(1)\text{-Cl}(1) = 2.6394(10)$; $\text{As}(1)\text{-Au}(1)\text{-As}(2) = 117.169(12)$; $\text{As}(1)\text{-Au}(1)\text{-As}(3) = 117.366(12)$; $\text{As}(2)\text{-Au}(1)\text{-As}(3) = 114.995(12)$; $\text{As}(1)\text{-Au}(1)\text{-Cl}(1) = 99.49(3)$; $\text{As}(2)\text{-Au}(1)\text{-Cl}(1) = 98.04(3)$; $\text{As}(3)\text{-Au}(1)\text{-Cl}(1) = 105.15(2)$. The structure has been deposited with Cambridge Crystallographic Data Centre (deposition number 2244690) and more detailed crystallographic data can be obtained free of charge. Detailed crystallographic data and refinement parameters are given in Table S1.

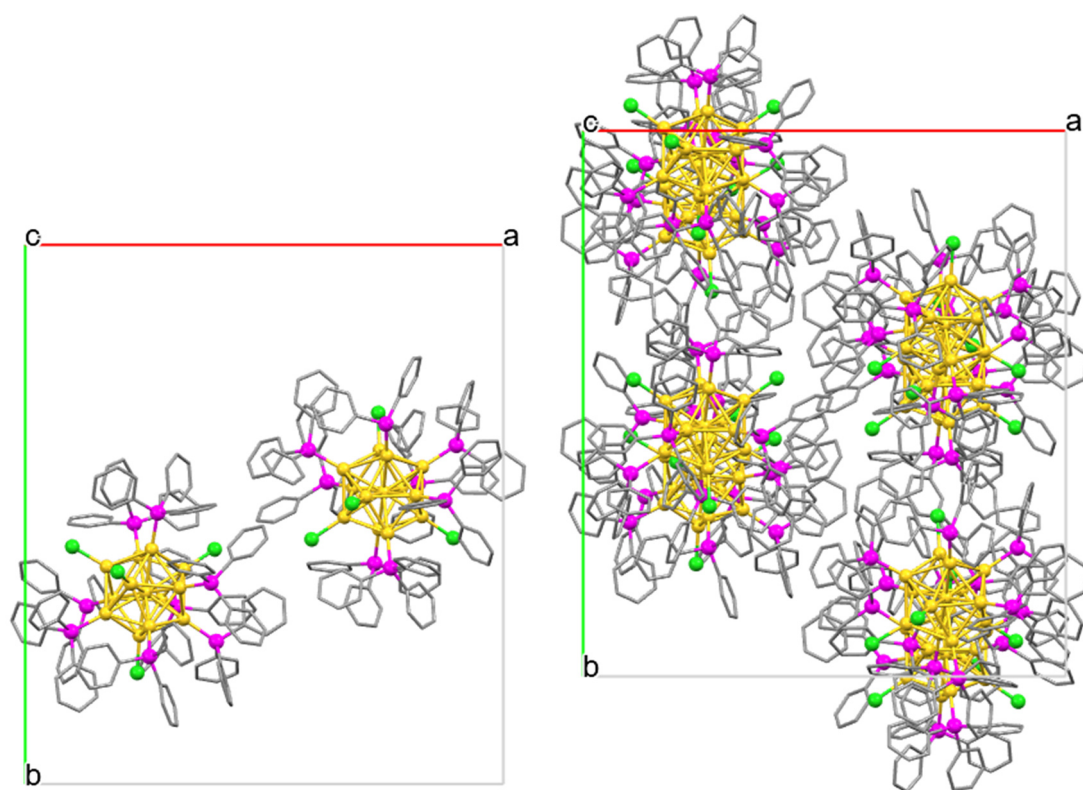


Figure S3. The two independent molecules of $\text{Au}_{13}\text{As}_8$ in the unit cell (left) and their stacking diagram (right).

Note: Detailed crystallographic data and refinement parameters, as well as the selected bond lengths and angles are given in Table S1. Color code: yellow, Au; magenta, As; green, Cl; grey, C. All hydrogen atoms are omitted for clarity.

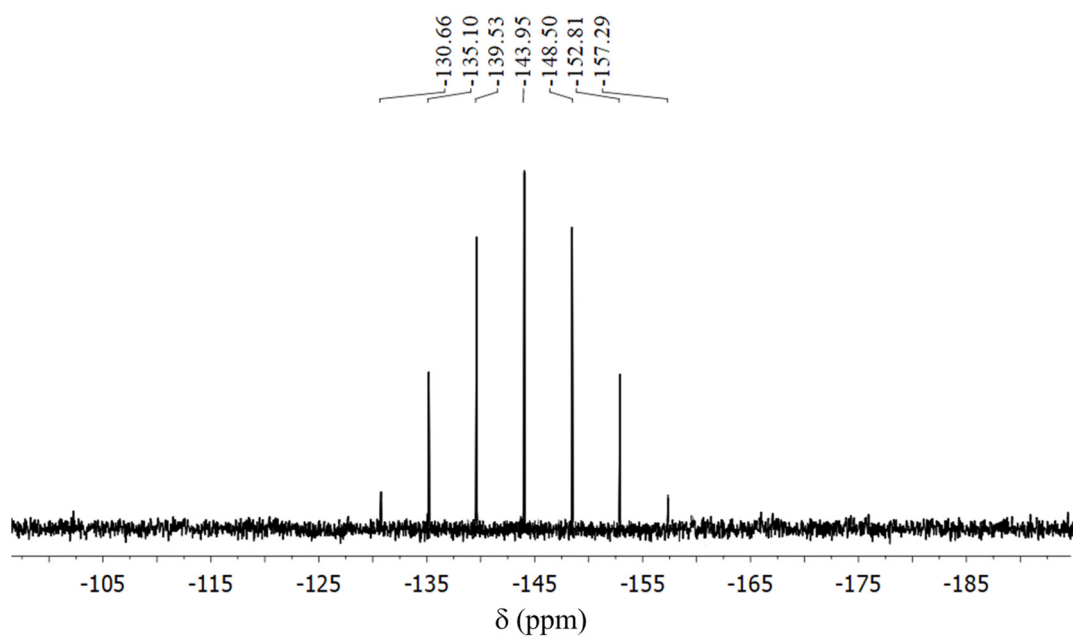


Figure S4. $^{31}\text{P}\{^1\text{H}\}$ NMR of $\text{Au}_{13}\text{As}_8$ in CD_2Cl_2 at room temperature.

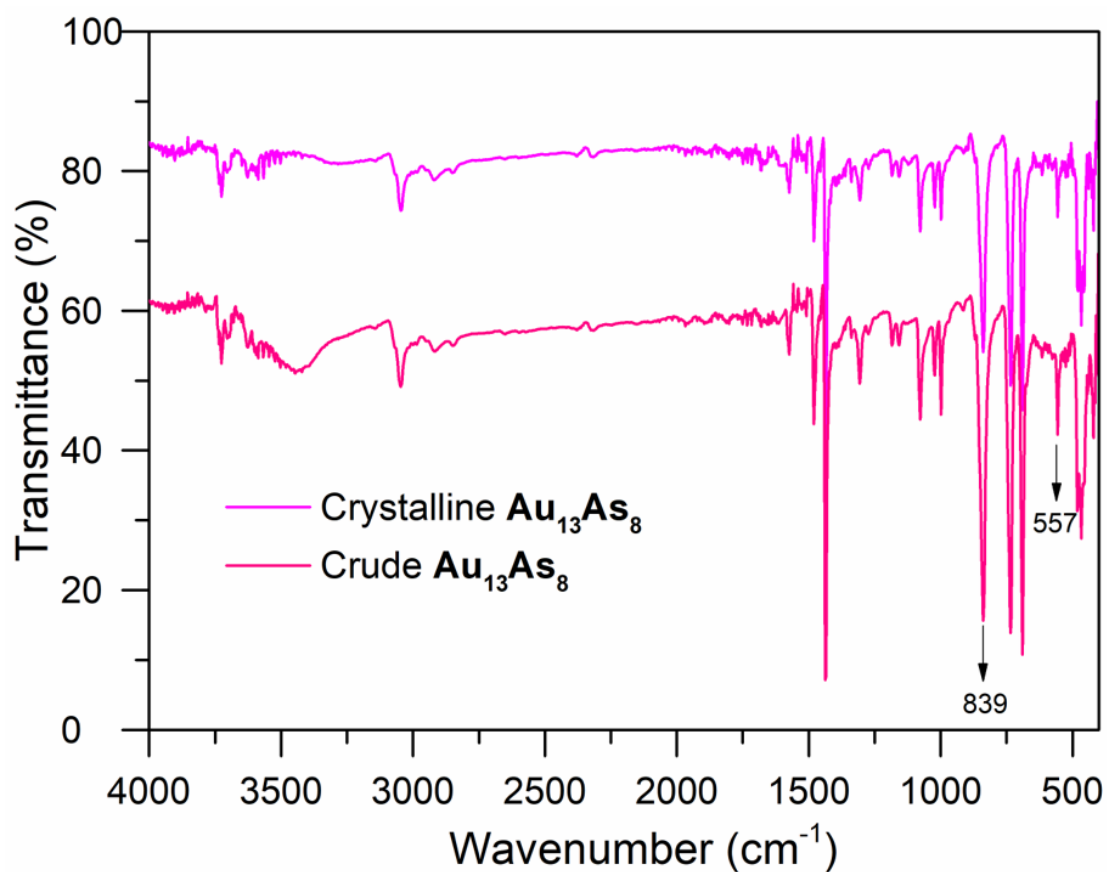


Figure S5. Compared IR spectra of crude and crystalline $\text{Au}_{13}\text{As}_8$.

Note: The vibrational peaks at 839 and 557 cm^{-1} are characteristic of PF_6^- .

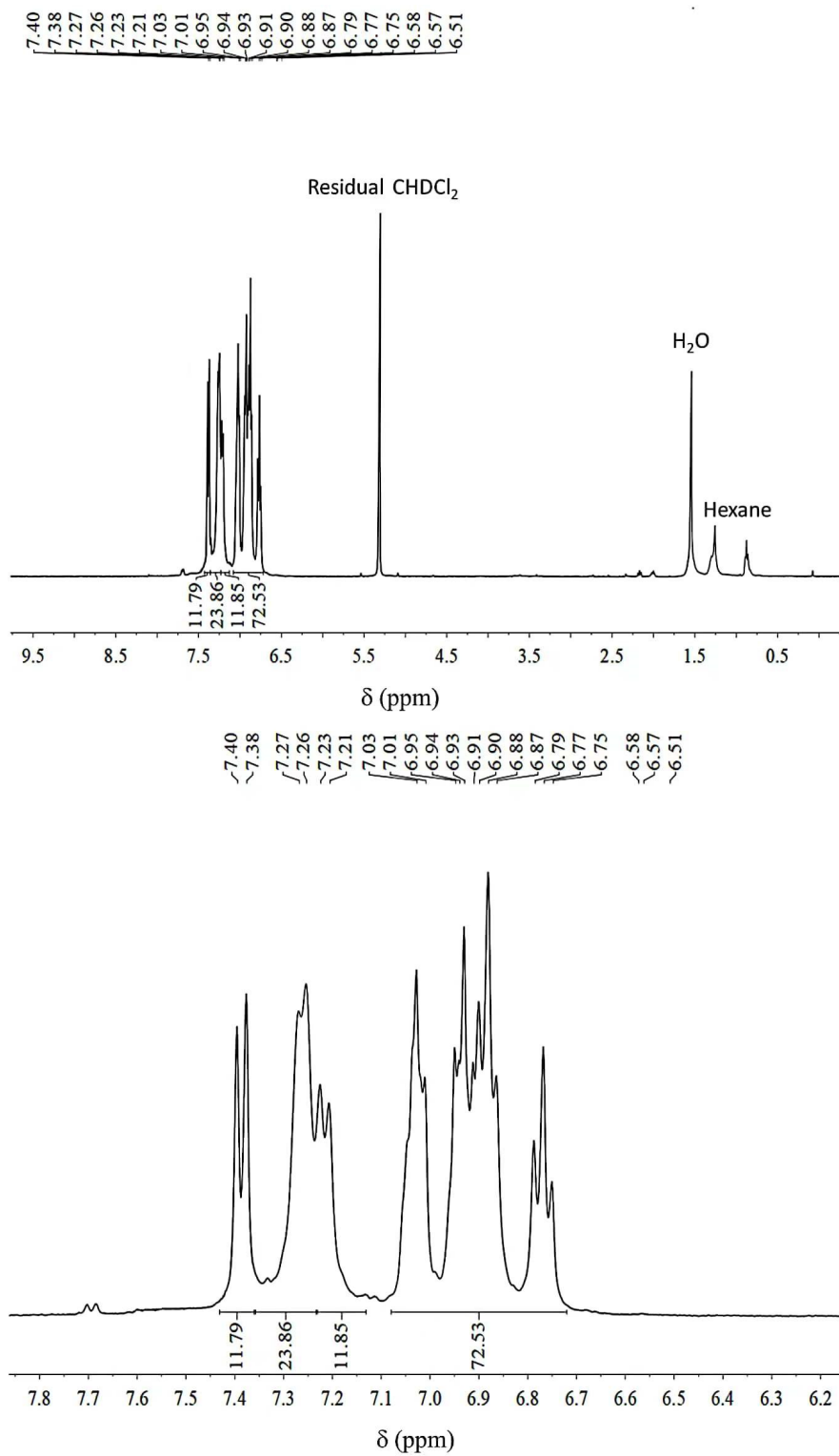


Figure S6. ^1H NMR of $\text{Au}_{13}\text{As}_8$ in CD_2Cl_2 at room temperature in full (top) and aromatic (bottom) regions.

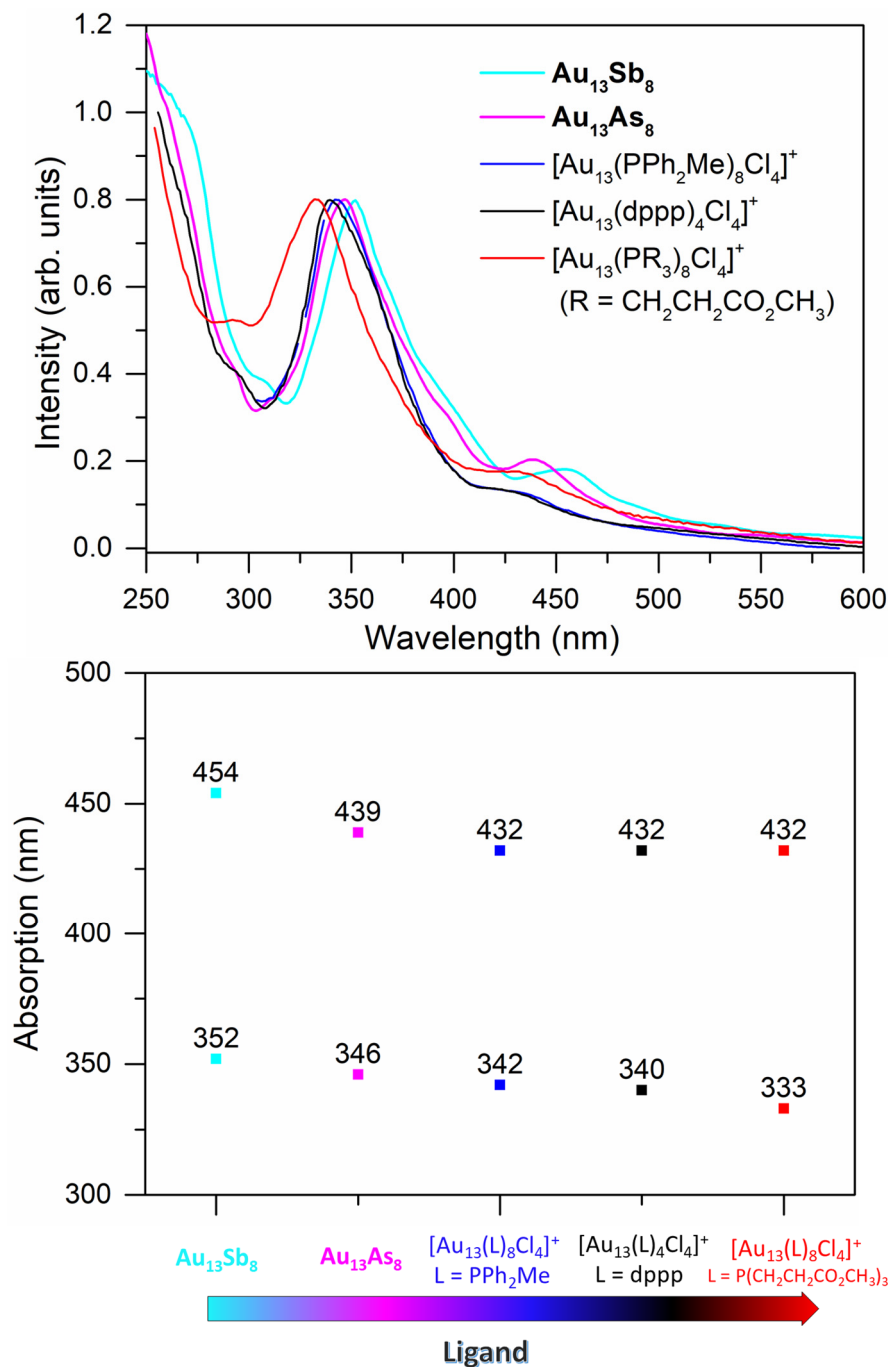


Figure S7. Experimental UV-vis spectra of $\text{Au}_{13}\text{As}_8$, $\text{Au}_{13}\text{Sb}_8$, $[\text{Au}_{13}(\text{PPh}_2\text{Me})_8\text{Cl}_4]^+$, $[\text{Au}_{13}(\text{dppp})_4\text{Cl}_4]^+$ (dppp = $\text{Ph}_2\text{P}(\text{CH}_2)_3\text{PPh}_2$) and $[\text{Au}_{13}(\text{PR}_3)_8\text{Cl}_4]^+$ ($\text{R} = \text{CH}_2\text{CH}_2\text{CO}_2\text{CH}_3$) (top), and correlations between ligands and absorptions (bottom).

Note: 1) The spectra of the latter three were abstracted from the corresponding literatures.^[16-18]

2) The spectrum of $[\text{Au}_{12}(\text{PR}_3)_8\text{Cl}_4]^+$ was recorded in $\text{CH}_2\text{Cl}_2/\text{CH}_3\text{OH}$ while others were in CH_2Cl_2 .

3) The exact structures of $[\text{Au}_{13}(\text{PPh}_2\text{Me})_8\text{Cl}_4]^+$ and $[\text{Au}_{13}(\text{dppp})_8\text{Cl}_4]^+$, or more precisely, their surface ligand arrangements, are unknown because they were only characterized spectroscopically.

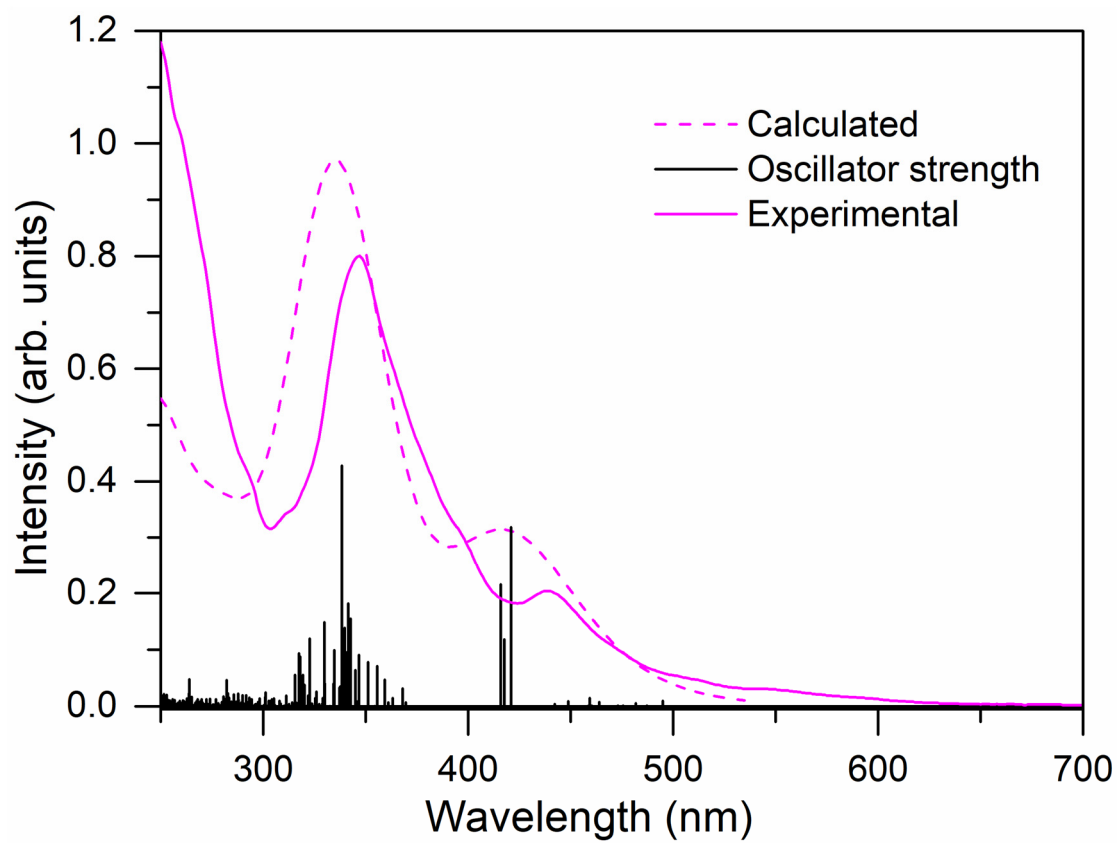


Figure S8. Experimental and TD-DFT calculated UV-vis spectra of Au₁₃As₈.

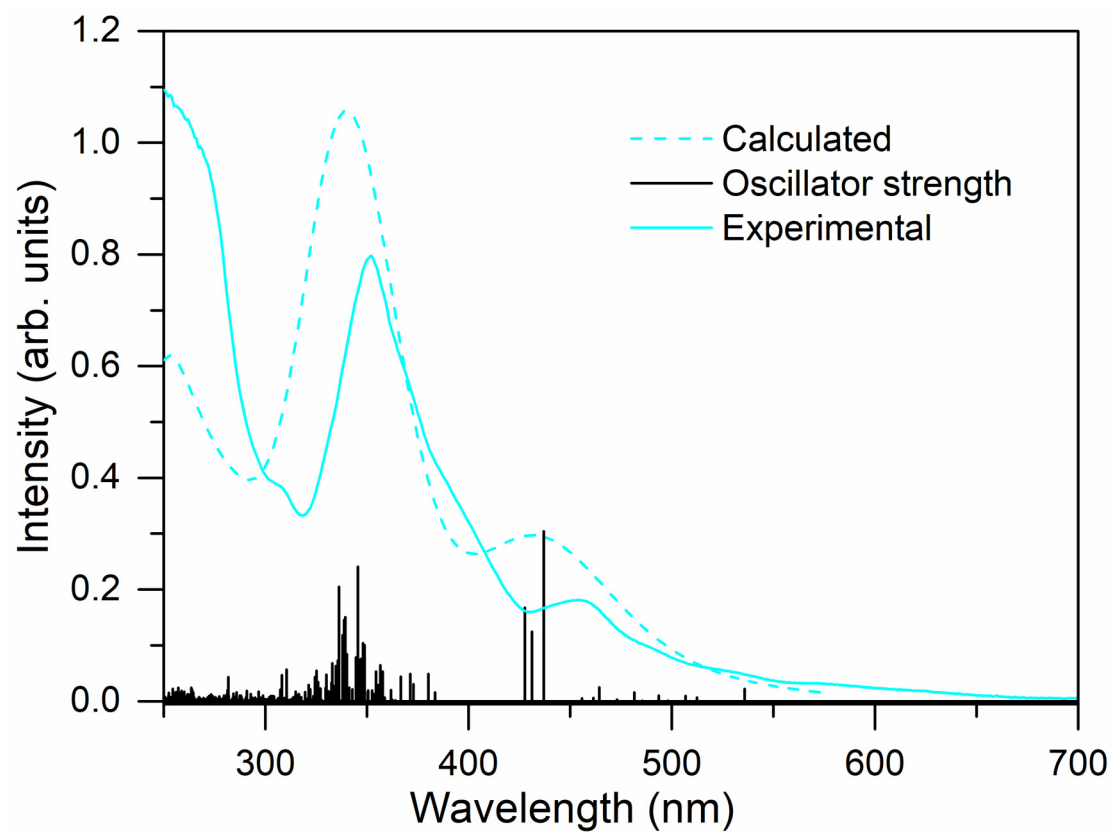


Figure S9. Experimental and TD-DFT calculated UV-vis spectra of $\text{Au}_{13}\text{Sb}_8$.

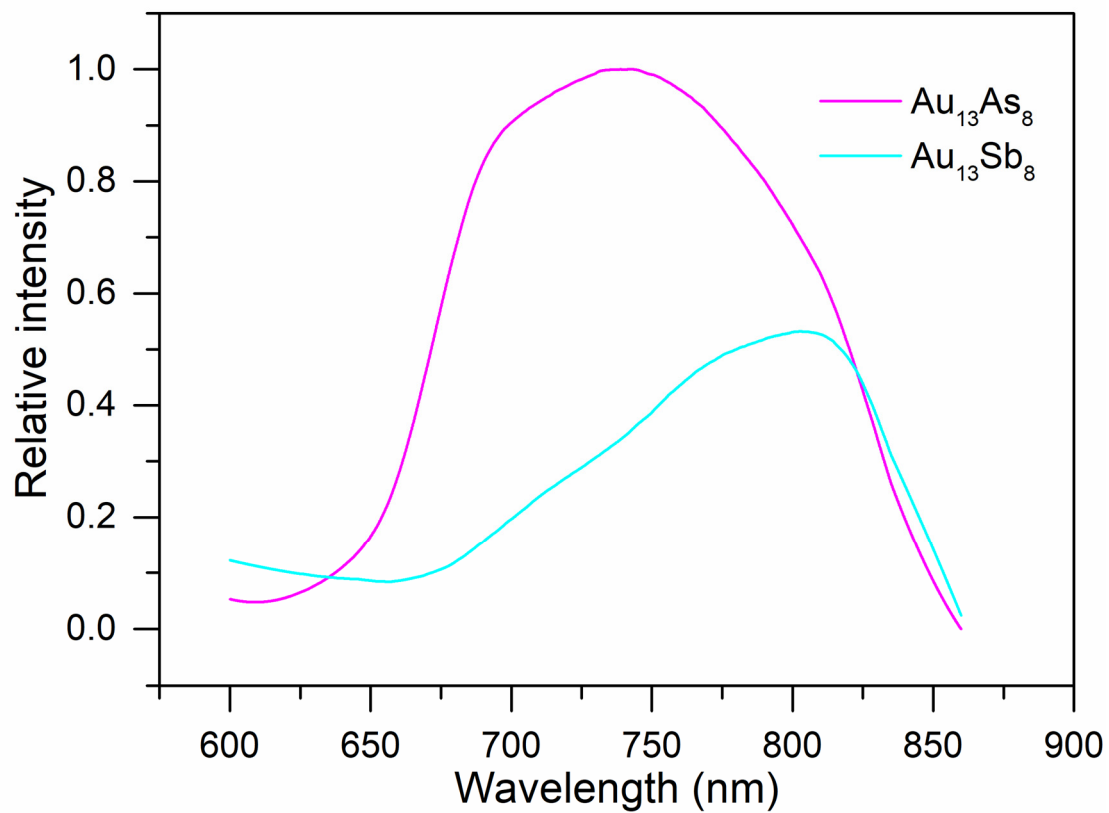


Figure S10. Photoluminescence spectra for $\text{Au}_{13}\text{As}_8$ (magenta line, $\lambda_{\text{ex}} = 460$ nm) and $\text{Au}_{13}\text{Sb}_8$ (cyan line, $\lambda_{\text{ex}} = 470$ nm) in crystalline state at room temperature.

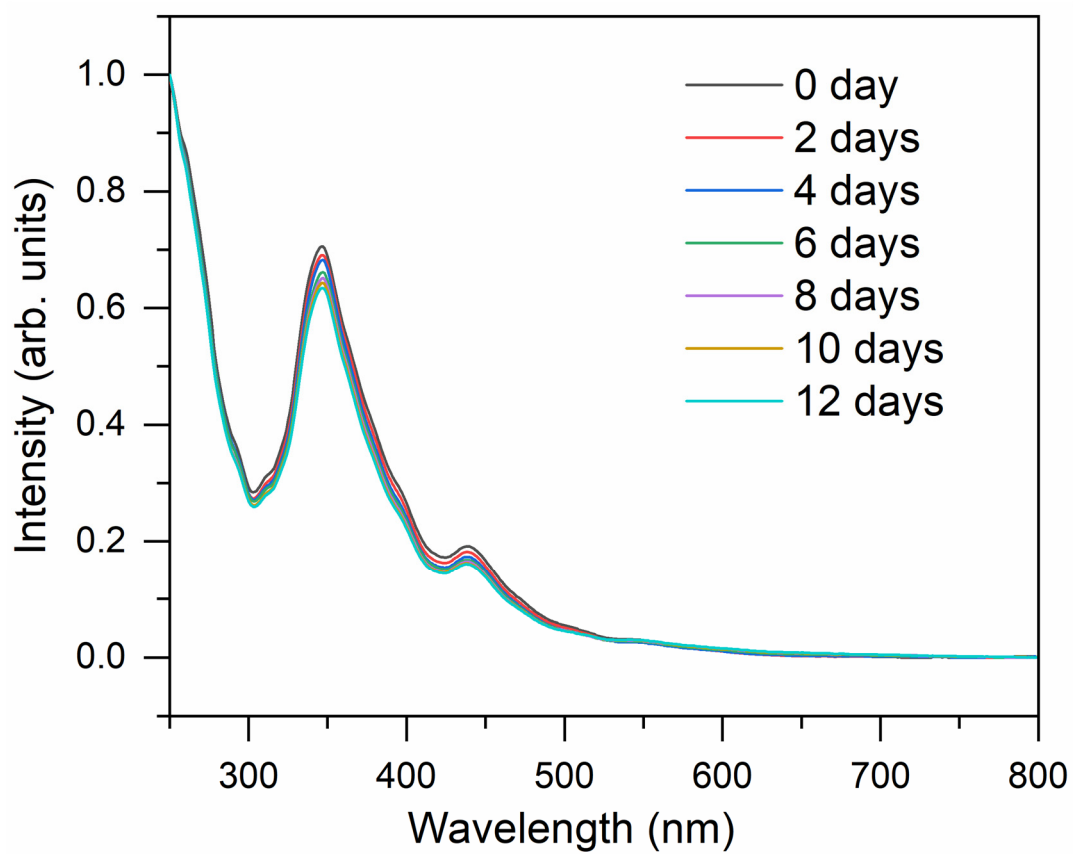


Figure S11. Time-course UV-vis spectra of Au₁₃As₈ in CH₂Cl₂ stored at 4 °C.

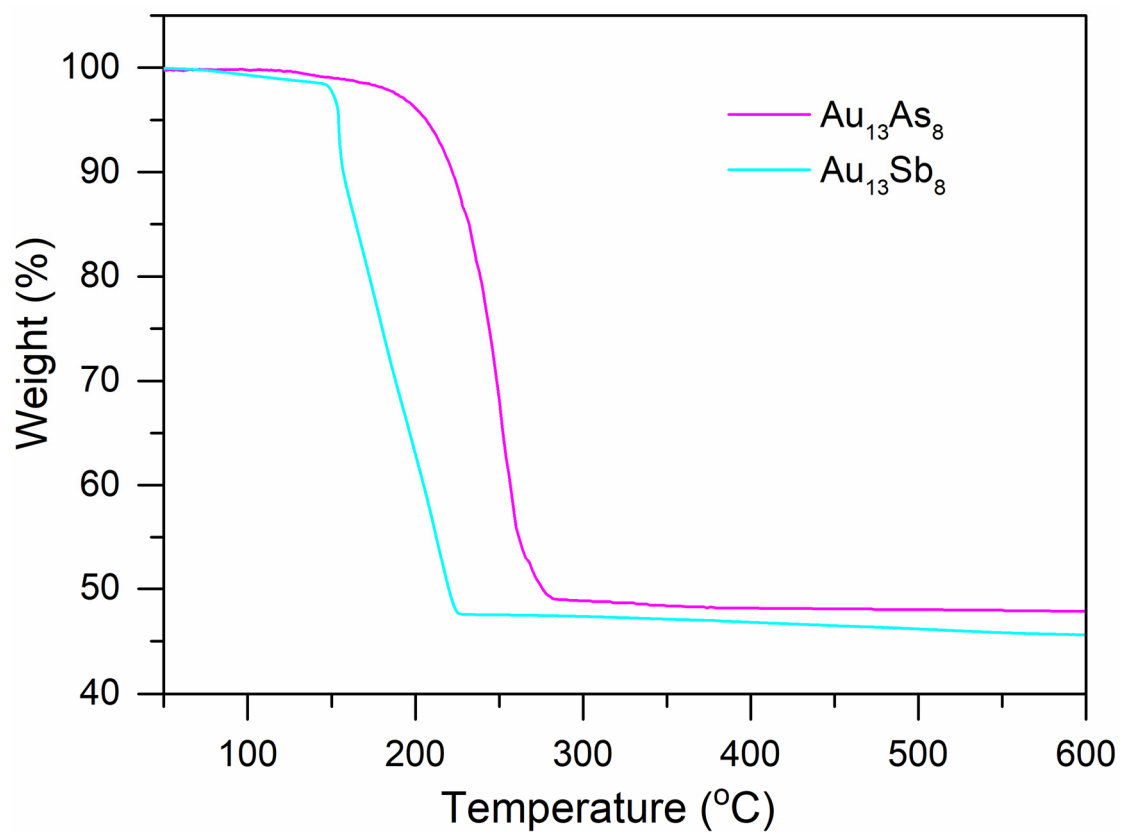


Figure S12. Compared TGA curves of **Au₁₃As₈** and **Au₁₃Sb₈**.

Note: The curve for **Au₁₃Sb₈** was abstracted from literature, ^[1] and the curve for **Au₁₃As₈** was acquired under the same conditions (heating rate: 10 °C/min; N₂ flow rate: 60 mL/min). For the **Au₁₃As₈** sample, the weight loss at 600 °C is *ca.* 47.9%, which corresponds to the loss of all ligands and is consistent with the theoretical value of 48.3%.

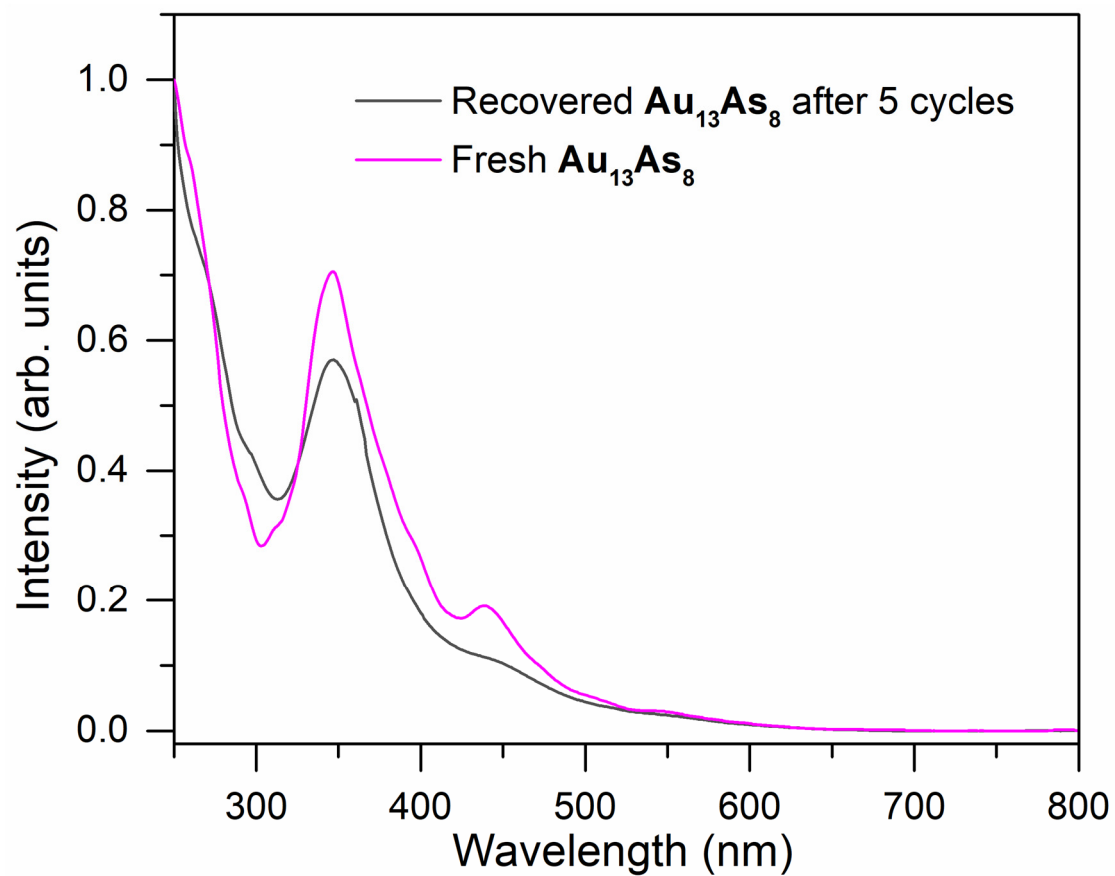


Figure S13. Compared UV-vis spectra of the fresh and recovered $\text{Au}_{13}\text{As}_8$ in DCM after five cycles.

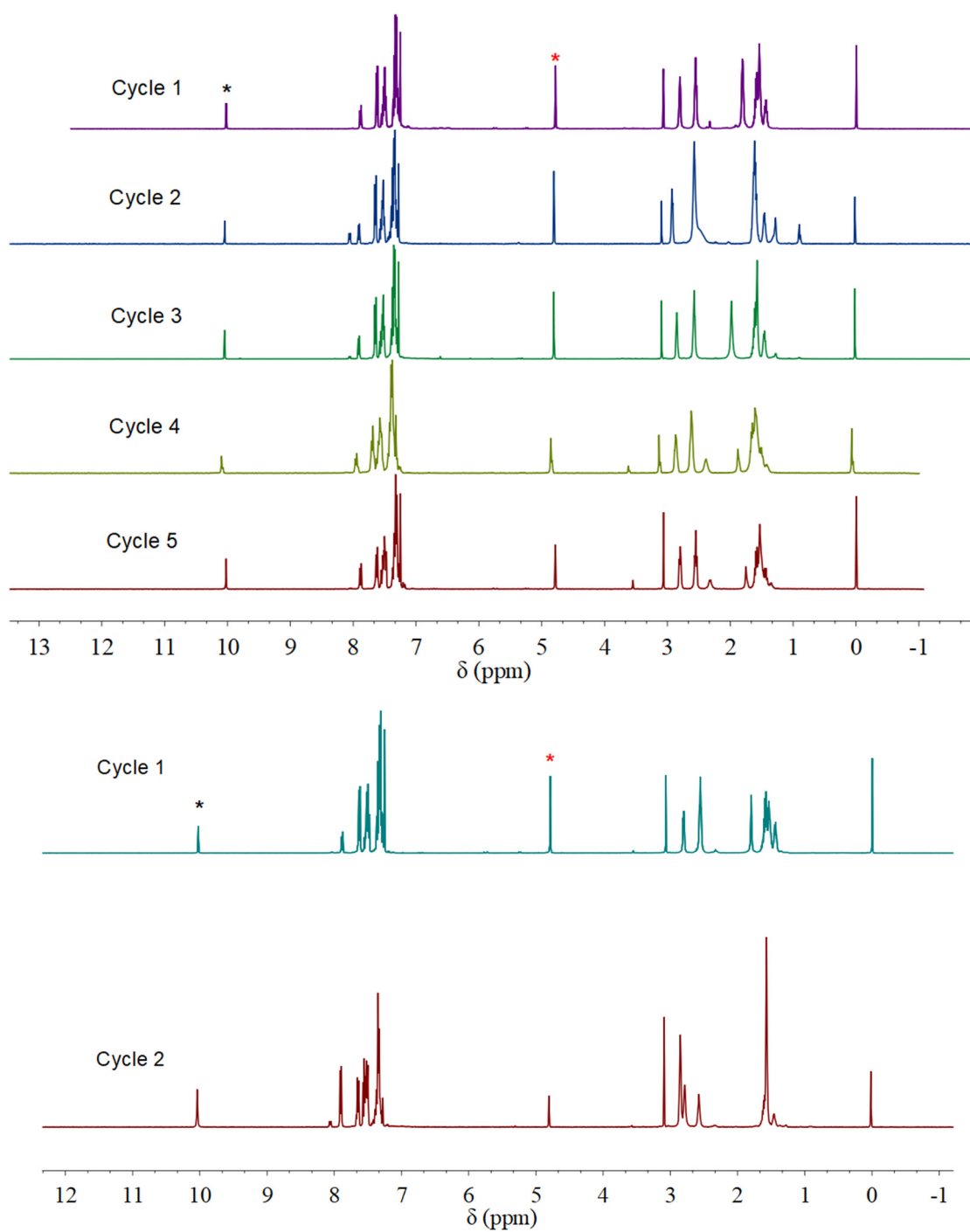


Figure S14. ¹H NMR of the crudes in CD₂Cl₂ for A³ coupling reactions catalyzed by Au₁₃As₈ (top) and Au₁₃Sb₈ (bottom).

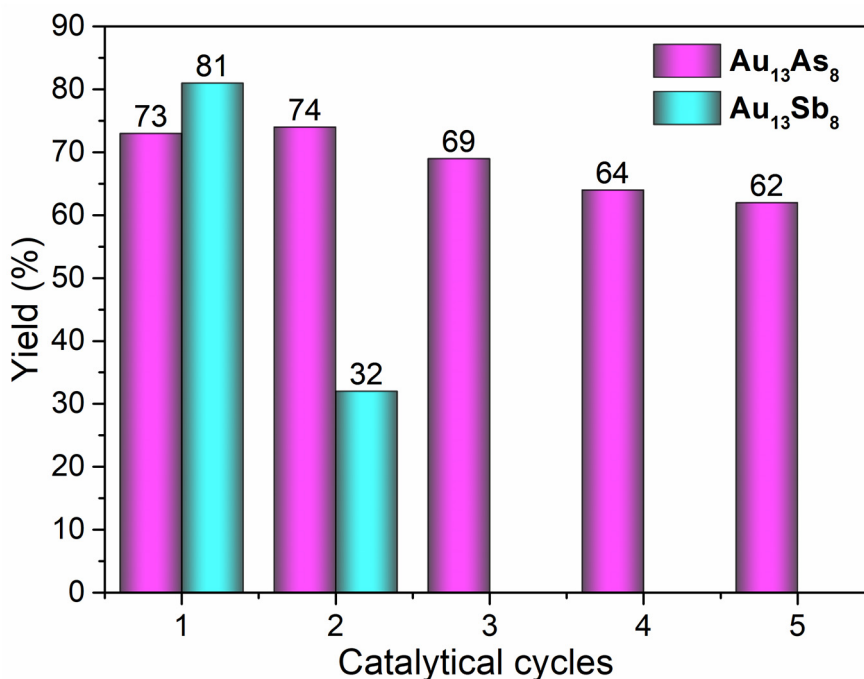
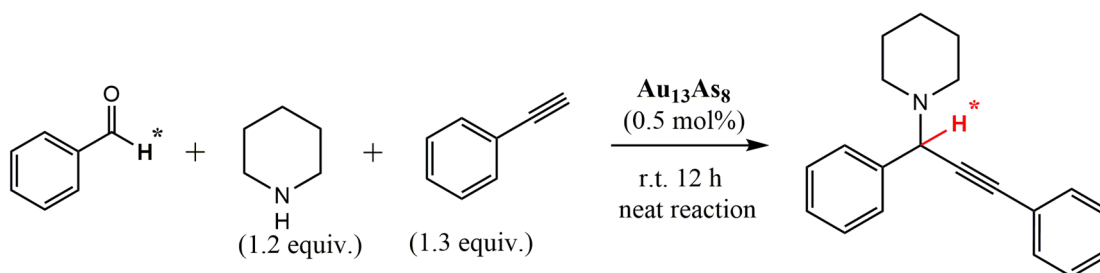


Figure S15. The NMR yields of propargylamine for the A^3 coupling reactions catalyzed by $\text{Au}_{13}\text{As}_8$ and $\text{Au}_{13}\text{Sb}_8$.

Note: 1) **Yield determination:** As shown in Figure S13 and the scheme below, the ^1H NMR resonances at 10.0 ppm (*) and 4.81 ppm (*) are assigned to benzaldehyde ($\text{HC}=\text{O}$) and propargylamine ($\text{C}-\text{H}$), respectively. Their relative integration ratios $\text{I}(\text{*})/[\text{I}(\text{*})+\text{I}(\text{*})]$ were used to determine the conversion ratio of benzaldehyde. Since there are no other side reactions observed, the conversion ratio of benzaldehyde was also used as the NMR yield of product.



2) **Catalytic performance comparison:** Under similar reaction conditions, the conversion ratio of benzaldehyde with $\text{Au}_{13}\text{Sb}_8$ as catalyst was determined to be *ca.* 81% in the first cycle, similar to the value (78%) reported in previous literature.^[14] Given the obvious decomposition observed in each cycle for $\text{Au}_{13}\text{Sb}_8$, no further trial was made after the second cycle due to the marked decrease in yield.

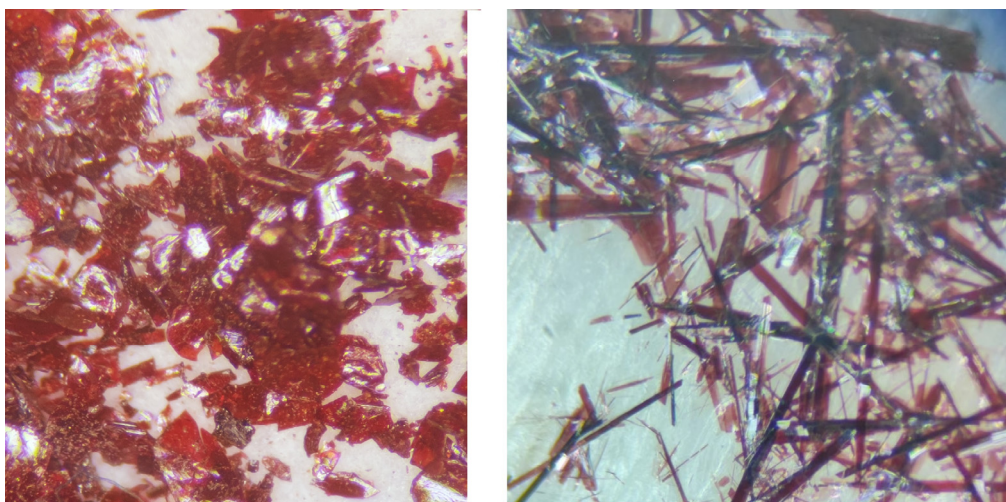


Figure S16. Photographs of the crystals of $[\text{Au}_{11}(\text{PPh}_3)_8\text{Cl}_2]^+$ (left) and $[\text{Au}_{13}(\text{dppe})_5\text{Cl}_2]^{3+}$ (right).

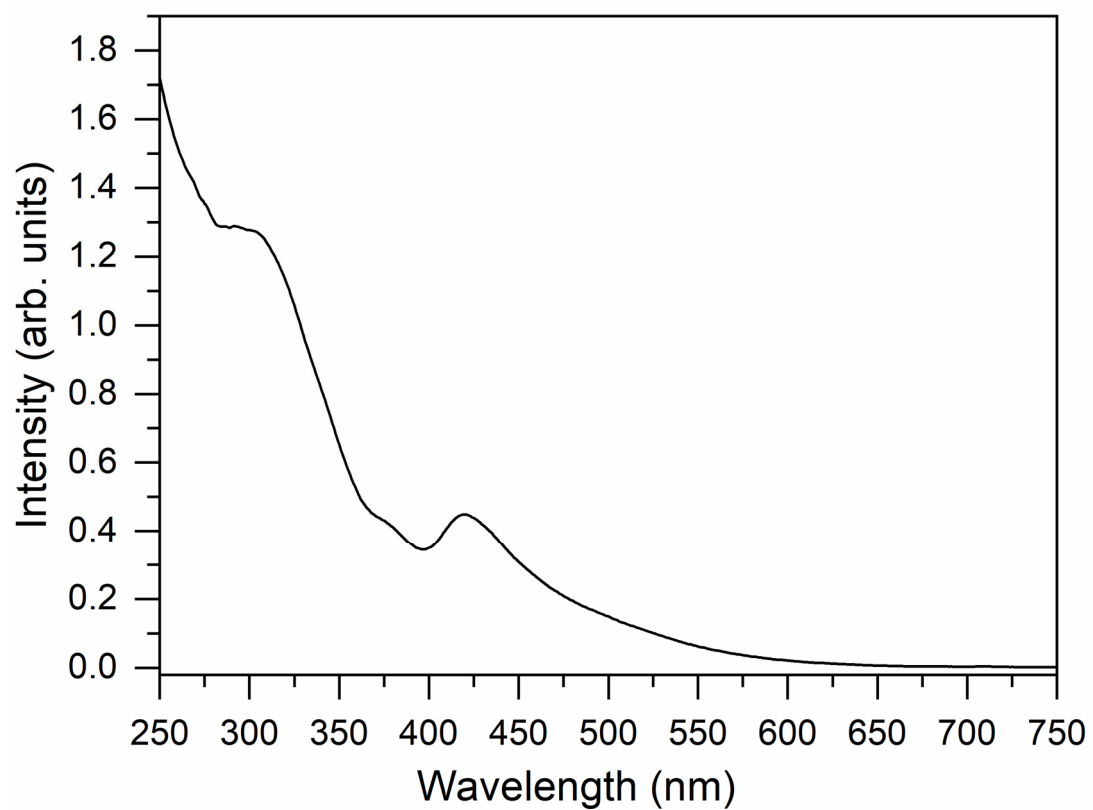


Figure S17. UV-vis spectrum of $[\text{Au}_{11}(\text{PPh}_3)_8\text{Cl}_2]^+$ in CH_2Cl_2 .

Note: The pattern and peak values are consistent with those from literature.^[19]

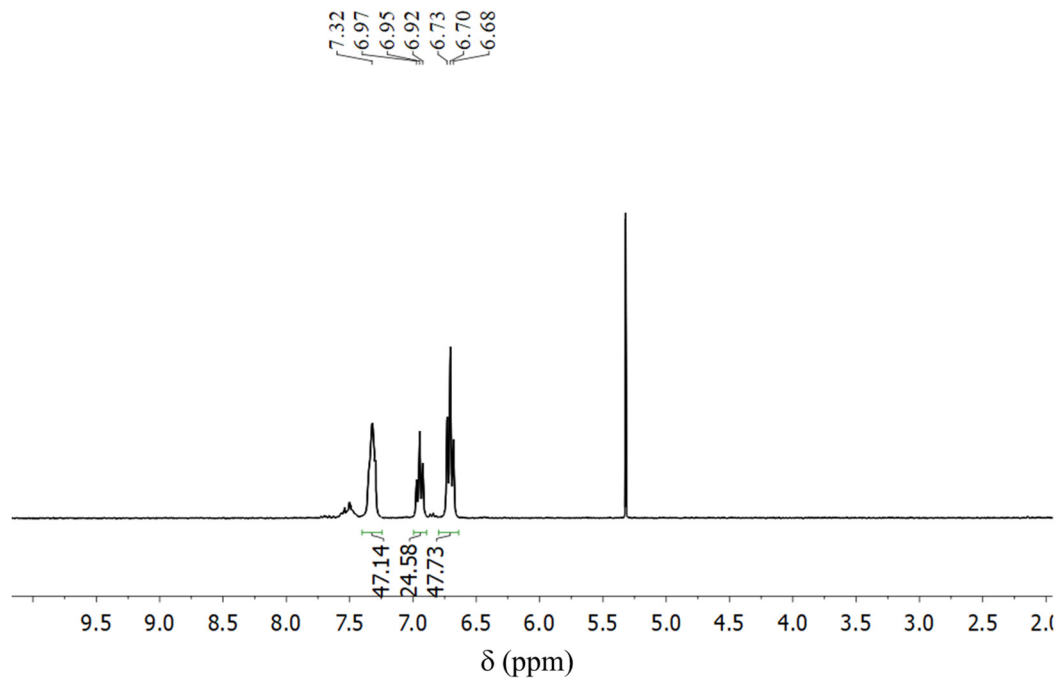


Figure S18. ${}^1\text{H}\{{}^{31}\text{P}\}$ NMR of $[\text{Au}_{11}(\text{PPh}_3)_8\text{Cl}_2]^+$ in CD_2Cl_2 .

Note: The pattern and peak values are consistent with those from literature.^[19]

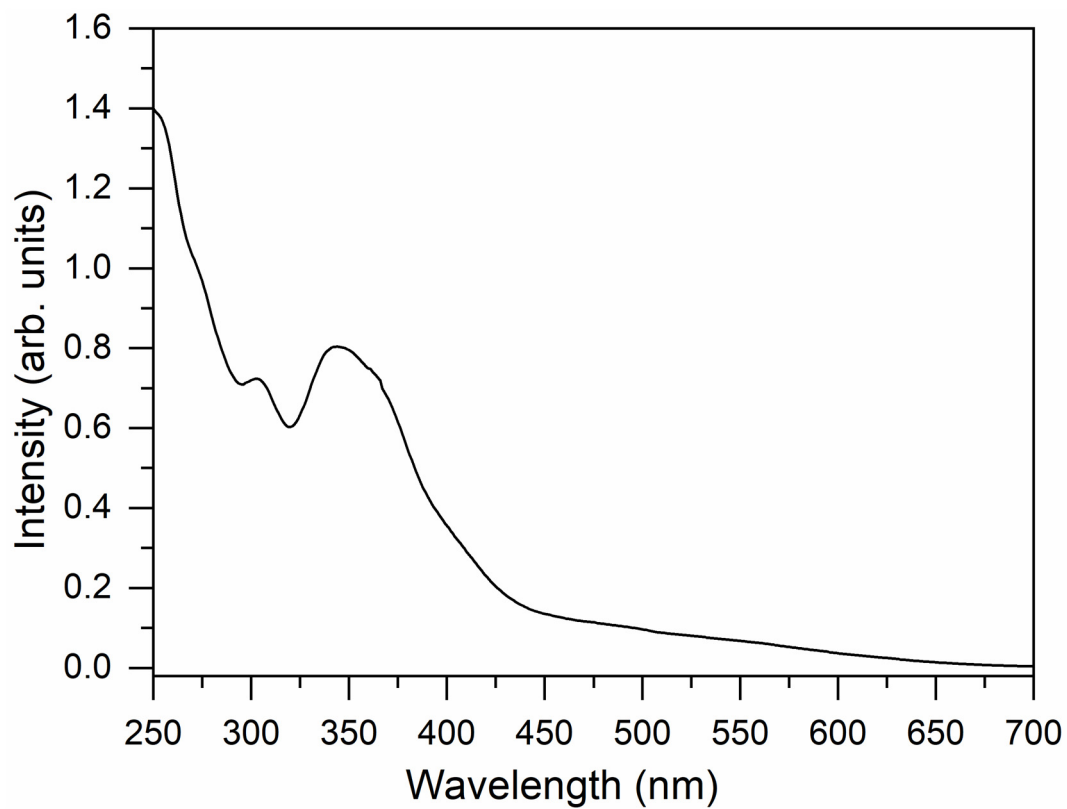


Figure S19. UV-vis spectrum of $[Au_{13}(dppe)_5Cl_2]^{3+}$ in CH_2Cl_2 .

Note: The pattern and peak values are consistent with those from literature.^[17]

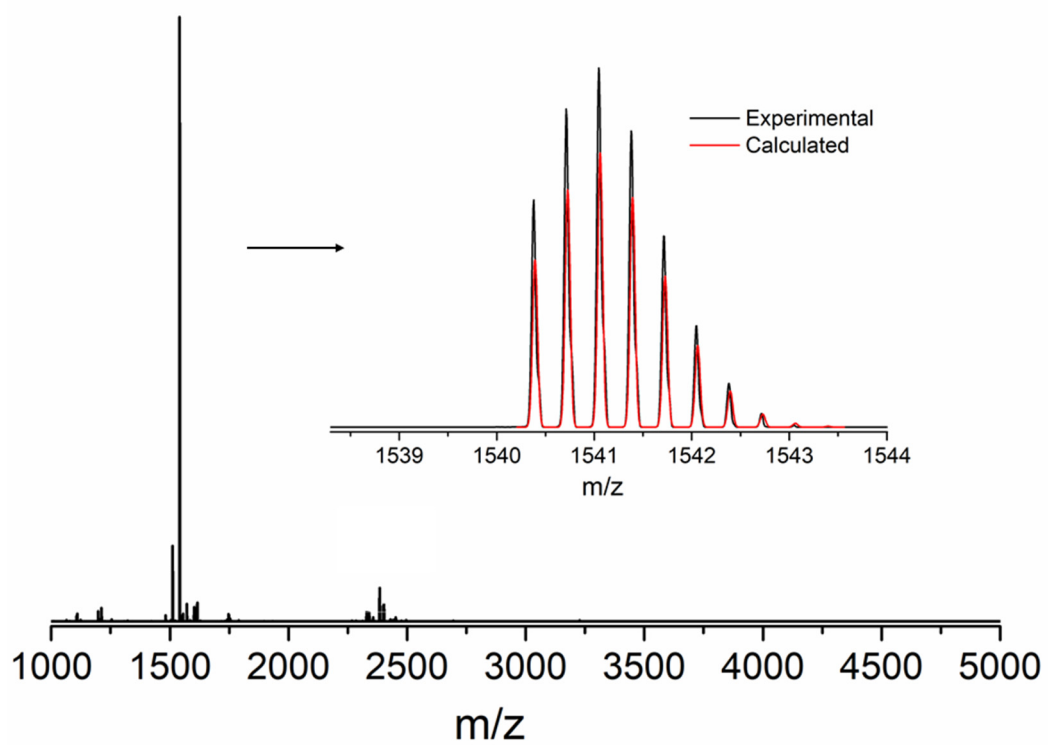


Figure S20. ESI-MS(+) spectrum of $[\text{Au}_{13}(\text{dppe})_5\text{Cl}_2]^{3+}$ in CH_2Cl_2 . Inset: the experimental (black trace) and calculated (red trace) isotopic patterns of the molecular ion $[\text{Au}_{13}(\text{dppe})_5\text{Cl}_2]^{3+}$.

Table S1. Crystallographic Data for **Au₁₃As₈** and **(Ph₃As)₃AuCl**.

Compound	Au₁₃As₈	(Ph₃As)₃AuCl
Empirical formula	C ₁₄₄ H ₁₂₀ As ₈ Au ₁₃ Cl ₄	C ₅₄ H ₄₅ As ₃ AuCl
Formula weight	5152.12	1151.07
Temperature/K	100(2)	100(2)
Crystal system	Monoclinic	Triclinic
Space group	P2 ₁ /n	P-1
a/Å	28.1786(2)	13.2861(4)
b/Å	31.8205(4)	13.9323(4)
c/Å	36.1804(5)	14.0077(4)
α/°	90	83.702(2)
β/°	91.8449(10)	75.517(3)
γ/°	90	86.706(2)
Volume/Å ³	32424.6(6)	2494.16(13)
Z	8	2
ρ _{calc} g/cm ³	2.111	1.533
Theta range for data collection	2.811 to 67.079°	3.275 to 67.075°
Absorption coefficient	24.229	8.491
F(000)	18744	1128
Radiation	Cu Kα (λ = 1.54184)	Cu Kα (λ = 1.54184)
Reflections collected	195960	25646
Independent reflections	57368 [R _{int} = 0.0919]	8779 [R _{int} = 0.0431]
Max. and min. transmission	1.00000 and 0.39067	1.00000 and 0.82453
Data/parameters	57368/2467	8779/532
Goodness-of-fit on F ²	1.077	1.055
Final R indexes [I > 2σ (I)]	R1 = 0.1337 wR2 = 0.3421	R1 = 0.0267 wR2 = 0.0650
Final R indexes [all data]	R1 = 0.1543 wR2 = 0.3562	R1 = 0.0288 wR2 = 0.0660
Largest diff. peak/hole / e Å ⁻³	5.060/-4.674	0.922/-1.012

Table S2. Selected bond distances (Å) for crystallographic $\text{Au}_{13}\text{As}_8$ and $\text{Au}_{13}\text{Sb}_8$.

$\text{Au}_{13}\text{As}_8$				$\text{Au}_{13}\text{Sb}_8$	
Independent molecule 1		Independent molecule 2			
Radial Au-Au bonds					
Bonded to As			Bonded to Sb		
Au1-Au3	2.759(2)	Au14-Au15	2.770(2)	Au13-Au1	2.794(2)
Au1-Au4	2.754(2)	Au14-Au17	2.757(2)	Au13-Au2	2.727(1)
Au1-Au7	2.807(2)	Au14-Au19	2.789(2)	Au13-Au3	2.737(1)
Au1-Au8	2.762(2)	Au14-Au20	2.745(2)	Au13-Au4	2.759(1)
Au1-Au9	2.810(2)	Au14-Au21	2.758(2)	Au13-Au5	2.715(1)
Au1-Au10	2.750(2)	Au14-Au23	2.766(2)	Au13-Au6	2.769(1)
Au1-Au11	2.760(2)	Au14-Au25	2.779(2)	Au13-Au7	2.722(1)
Au1-Au12	2.739(2)	Au14-Au26	2.758(2)	Au13-Au8	2.727(1)
<i>Sub-Average</i>	<i>2.766(2)</i>	<i>Sub-Average</i>	<i>2.765(2)</i>	<i>Sub-Average</i>	<i>2.744(2)</i>
Bonded to Cl			Bonded to Cl		
Au1-Au2	2.726(2)	Au14-Au16	2.737(2)	Au13-Au9	2.756(1)
Au1-Au5	2.750(2)	Au14-Au18	2.736(2)	Au13-Au10	2.763(1)
Au1-Au6	2.739(2)	Au14-Au22	2.734(2)	Au13-Au11	2.735(1)
Au1-Au13	2.730(2)	Au14-Au24	2.757(2)	Au13-Au12	2.766(1)
<i>Sub-Average</i>	<i>2.736(2)</i>	<i>Sub-Average</i>	<i>2.741(2)</i>	<i>Sub-Average</i>	<i>2.755(2)</i>
<i>Average</i>	<i>2.757(2)</i>	<i>Average</i>	<i>2.757(2)</i>	<i>Average</i>	<i>2.748(1)</i>
Peripheral Au-Au bonds					
Au2-Au3	2.886(2)	Au15-Au16	2.905(3)	Au1-Au6	2.910(1)
Au2-Au4	2.861(2)	Au15-Au17	2.903(2)	Au1-Au7	2.862(1)
Au2-Au7	2.898(2)	Au15-Au18	2.838(2)	Au1-Au11	2.908(2)
Au2-Au8	2.878(2)	Au15-Au19	2.918(2)	Au2-Au9	2.868(1)
Au2-Au12	2.939(2)	Au15-Au20	2.956(2)	Au2-Au10	2.910(1)
Au3-Au4	2.961(3)	Au16-Au17	2.905(2)	Au2-Au3	2.893(1)
Au3-Au5	2.923(2)	Au16-Au20	2.846(2)	Au2-Au1	2.917(1)
Au3-Au6	2.812(2)	Au16-Au21	2.962(2)	Au2-Au11	2.840(1)
Au3-Au7	2.906(2)	Au16-Au25	2.890(2)	Au3-Au8	2.869(1)
Au4-Au5	2.830(2)	Au17-Au18	2.910(2)	Au3-Au9	2.925(1)
Au4-Au8	2.909(2)	Au17-Au24	2.824(2)	Au3-Au10	2.849(1)
Au4-Au9	2.907(2)	Au17-Au25	2.935(3)	Au3-Au4	2.886(1)
Au5-Au6	2.905(2)	Au18-Au19	2.968(2)	Au4-Au5	2.877(1)
Au5-Au9	2.955(2)	Au18-Au23	2.808(2)	Au4-Au12	2.886(1)
Au5-Au10	2.831(2)	Au18-Au24	2.901(2)	Au5-Au6	2.876(2)
Au6-Au7	2.985(2)	Au19-Au20	2.842(2)	Au5-Au11	2.896(2)
Au6-Au10	2.909(2)	Au19-Au22	2.890(2)	Au5-Au12	2.884(1)
Au6-Au11	2.836(2)	Au19-Au23	2.932(2)	Au6-Au7	2.906(1)
Au7-Au11	2.916(2)	Au20-Au21	2.889(2)	Au6-Au11	2.855(1)
Au7-Au12	2.870(2)	Au20-Au22	2.963(2)	Au6-Au12	2.895(1)
Au8-Au9	2.861(2)	Au21-Au22	2.851(2)	Au7-Au12	2.855(2)

Au8-Au12	2.904(2)	Au21-Au25	2.872(2)	Au8-Au9	2.864(1)
Au8-Au13	2.934(2)	Au21-Au26	2.940(2)	Au8-Au4	2.845(1)
Au9-Au10	2.908(2)	Au22-Au23	2.882(2)	Au8-Au7	2.898(1)
Au9-Au13	2.909(2)	Au22-Au26	2.887(2)	Au8-Au12	2.953(1)
Au10-Au11	2.955(2)	Au23-Au24	2.955(2)	Au9-Au1	2.916(1)
Au10-Au13	2.901(2)	Au23-Au26	2.940(2)	Au9-Au7	2.919(1)
Au11-Au12	2.942(2)	Au24-Au25	2.947(2)	Au10-Au4	2.957(1)
Au11-Au13	2.910(2)	Au24-Au26	2.841(2)	Au10-Au5	2.850(1)
Au12-Au13	2.850(2)	Au25-Au26	2.898(2)	Au10-Au11	2.905(1)
Average	2.900(2)	Average	2.900(2)	Average	2.889(1)
Au-As or Au-Sb bonds					
Au10-As1	2.397(4)	Au17-As9	2.398(4)	Au1-Sb1	2.539(2)
Au9-As2	2.414(4)	Au15-As10	2.412(5)	Au2-Sb2	2.524(2)
Au3-As3	2.396(4)	Au19-As11	2.417(4)	Au3-Sb3	2.522(2)
Au7-As4	2.414(6)	Au23-As12	2.390(4)	Au4-Sb4	2.547(2)
Au12-As5	2.400(4)	Au26-As13	2.407(4)	Au5-Sb5	2.518(2)
Au8-As6	2.399(5)	Au21-As14	2.402(4)	Au6-Sb6	2.532(2)
Au4-As7	2.392(4)	Au25-As15	2.408(5)	Au7-Sb7	2.521(2)
Au11-As8	2.407(4)	Au20-As16	2.388(4)	Au8-Sb8	2.523(2)
Average	2.402(4)	Average	2.403(4)	Average	2.528(2)
Au-Cl bonds					
Au2-Cl1	2.37(1)	Au16-Cl5	2.32(1)	Au9-Cl1	2.350(5)
Au5-Cl2	2.31(1)	Au18-Cl6	2.32(2)	Au10-Cl2	2.327(7)
Au6-Cl3	2.331(9)	Au24-Cl7	2.350(9)	Au11-Cl3	2.298(6)
Au13-Cl4	2.333(9)	Au22-Cl8	2.332(9)	Au12-Cl4	2.353(5)
Average	2.34(1)	Average	2.33(1)	Average	2.332(6)

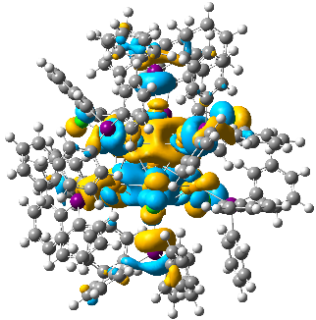
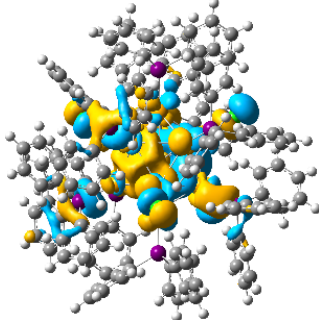
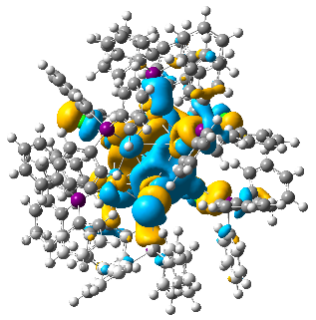
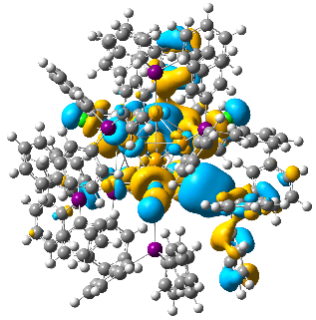
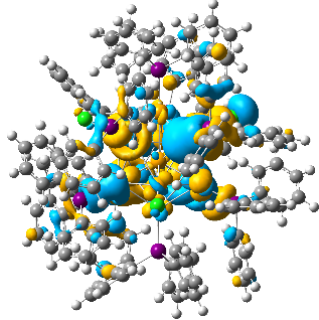
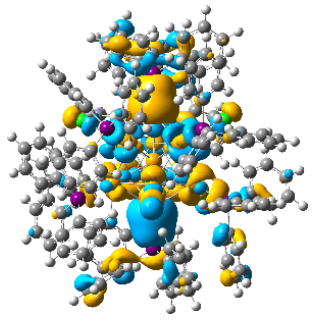
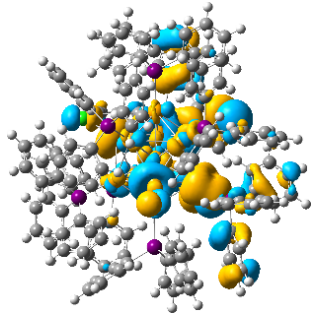
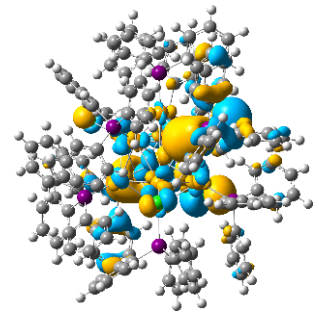
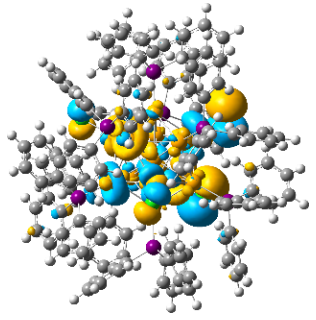
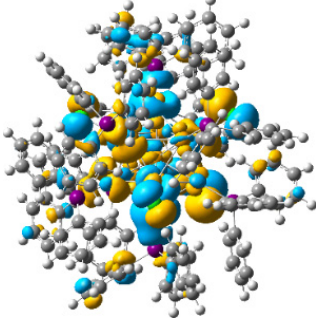
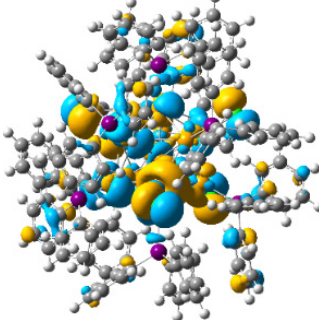
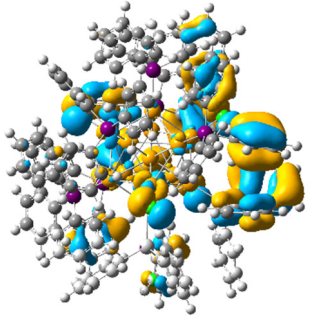
Note: The comparison data for **Au₁₃Sb₈** was abstracted from literature.^[11]

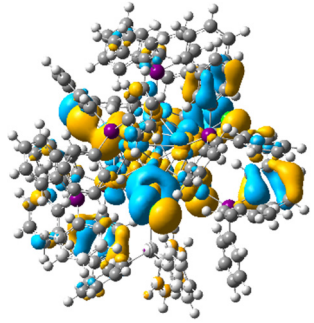
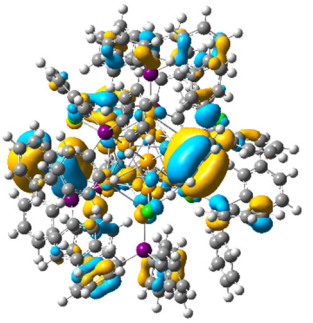
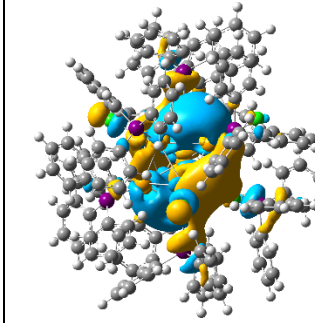
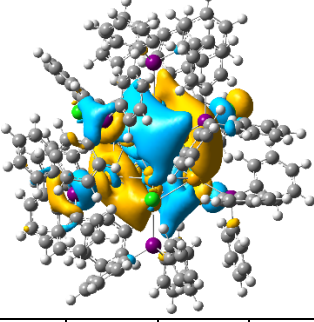
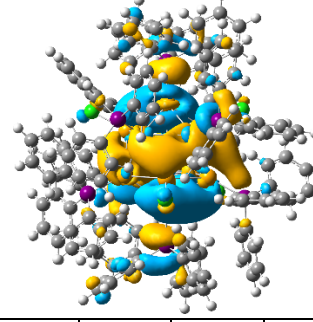
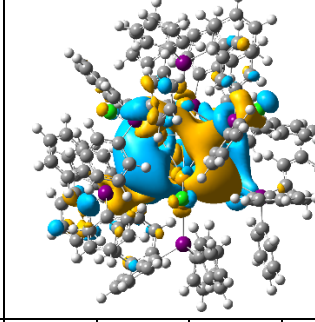
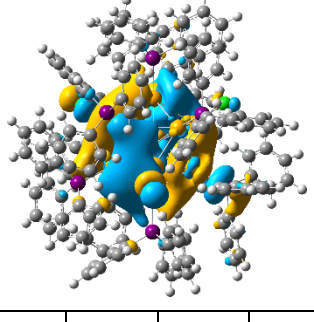
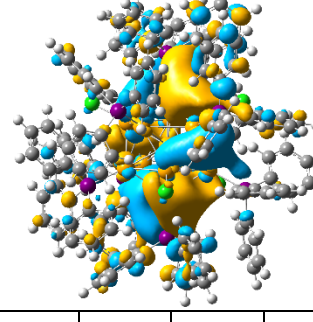
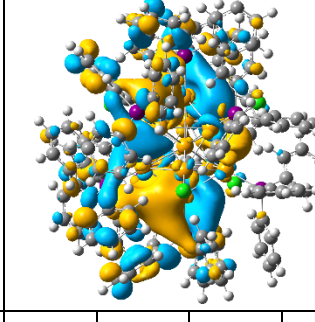
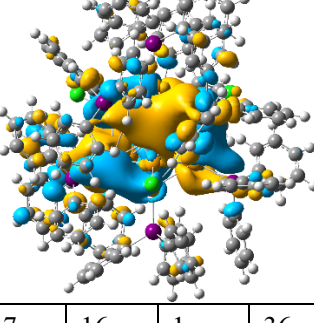
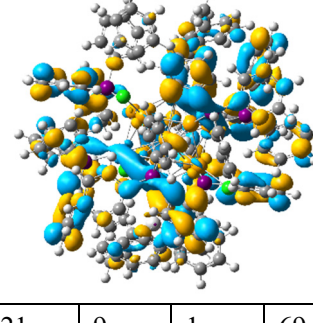
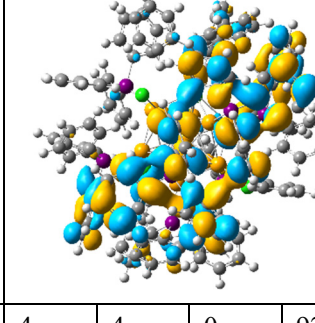
Table S3. Selected bond distances (Å) for structurally optimized **Au₁₃As₈** and **Au₁₃Sb₈**.

Au₁₃As₈				Au₁₃Sb₈			
Radial Au-Au bonds							
Bonded to As	Au1-Au2	2.85716	Bonded to Sb	Au6-Au1	2.82279		
	Au1-Au3	2.86254		Au6-Au2	2.82895		
	Au1-Au4	2.88361		Au6-Au3	2.81448		
	Au1-Au5	2.82639		Au6-Au13	2.85363		
	Au1-Au7	2.82639		Au6-Au14	2.85194		
	Au1-Au8	2.88360		Au6-Au15	2.82930		
	Au1-Au9	2.85716		Au6-Au16	2.84249		
	Au1-Au12	2.86253		Au6-Au17	2.80417		
	<i>Sub-Average</i>	<i>2.85742</i>		<i>Sub-Average</i>	<i>2.83097</i>		
Bonded to Cl	Au1-Au6	2.78475	Bonded to Cl	Au6-Au4	2.77441		
	Au1-Au10	2.81380		Au6-Au5	2.79928		
	Au1-Au11	2.81380		Au6-Au18	2.80029		
	Au1-Au13	2.78475		Au6-Au19	2.78283		
	<i>Sub-Average</i>	<i>2.79928</i>		<i>Sub-Average</i>	<i>2.78920</i>		
Average	2.83804		Average	2.81705			
Peripheral Au-Au bonds							
Au6-Au2		2.97994	Au19-Au3		2.98191		
Au6-Au3		2.98150	Au19-Au17		2.94184		
Au6-Au4		2.98171	Au19-Au16		2.94452		
Au6-Au5		2.96298	Au19-Au15		2.95804		
Au6-Au7		3.00875	Au19-Au14		2.95433		
Au9-Au8		3.02612	Au3-Au17		3.00807		
Au9-Au10		2.99068	Au17-Au16		2.98701		
Au9-Au11		2.90047	Au16-Au15		2.97290		
Au9-Au12		3.01108	Au15-Au14		2.97639		
Au9-Au13		2.97994	Au14-Au3		2.94415		
Au5-Au7		3.02026	Au17-Au13		2.93517		
Au7-Au4		2.96895	Au13-Au16		3.01323		
Au4-Au2		3.02613	Au16-Au18		2.91179		
Au2-Au3		3.01108	Au18-Au15		2.96689		
Au3-Au5		3.02421	Au18-Au5		2.88812		
Au5-Au13		3.00874	Au5-Au14		3.00365		
Au13-Au7		2.96297	Au14-Au2		2.97782		
Au7-Au12		3.02421	Au2-Au3		2.98728		
Au12-Au4		3.01212	Au3-Au4		2.93665		

Au4-Au10	2.98637	Au4-Au17	2.98738
Au10-Au2	2.90046	Au1-Au5	2.94961
Au2-Au11	2.99068	Au1-Au18	2.90939
Au11-Au3	2.93193	Au1-Au13	2.98948
Au3-Au8	3.01213	Au1-Au4	2.96830
Au8-Au5	2.96896	Au1-Au2	2.99319
Au10-Au11	2.98003	Au2-Au5	2.94333
Au10-Au12	2.93193	Au5-Au18	2.94156
Au12-Au13	2.98151	Au18-Au13	2.96830
Au13-Au8	2.98171	Au13-Au4	2.97509
Au8-Au11	2.98637	Au4-Au2	2.95298
Average	2.98446	Average	2.96228
Au-As or Au-Sb bonds			
Au12-As17	2.47532	Au3-Sb12	2.62274
Au8-As21	2.48352	Au17-Sb21	2.61857
Au9-As16	2.45718	Au16-Sb11	2.62423
Au3-As14	2.47532	Au15-Sb20	2.60637
Au5-As19	2.46736	Au14-Sb10	2.63306
Au7-As20	2.46736	Au2-Sb9	2.62853
Au4-As18	2.48352	Au13-Sb7	2.63614
Au2-As15	2.45718	Au1-Sb8	2.61536
Average	2.47134	Average	2.62313
Au-Cl bonds			
Au13-Cl24	2.43240	Au19-Cl25	2.47519
Au11-Cl22	2.41028	Au4-Cl22	2.47801
Au10-Cl23	2.41028	Au18-Cl24	2.45727
Au6-Cl168	2.43240	Au5-Cl23	2.45714
Average	2.42134	Average	2.46690

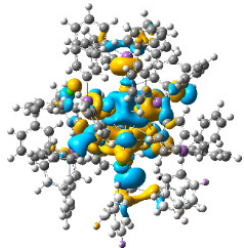
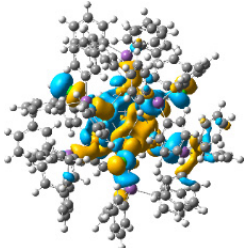
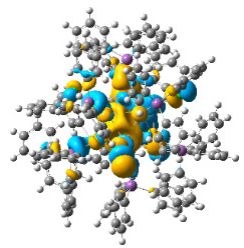
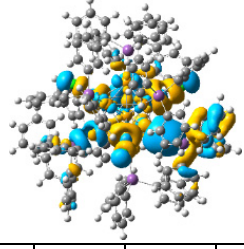
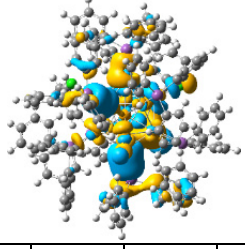
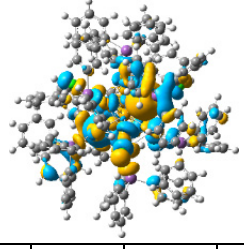
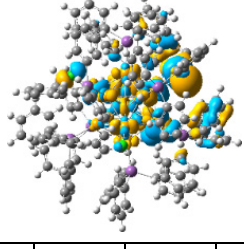
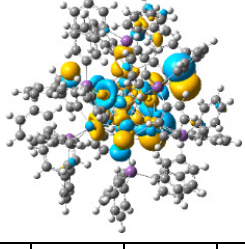
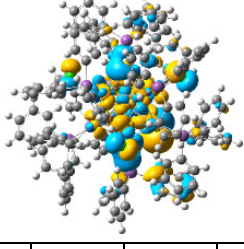
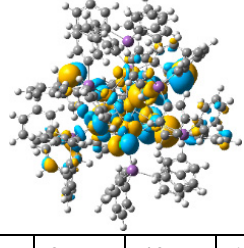
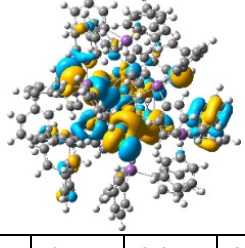
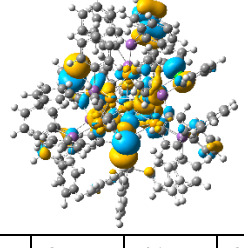
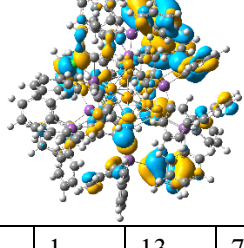
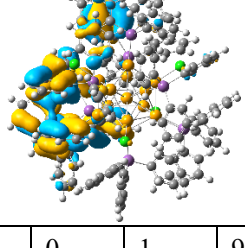
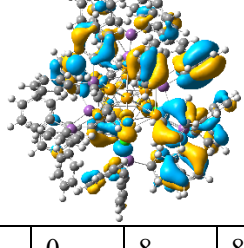
Table S4. Selected orbitals of $\text{Au}_{13}\text{As}_8$ and elemental contribution ratios (%).

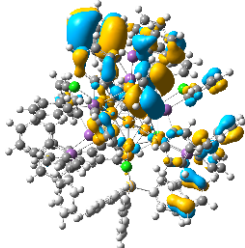
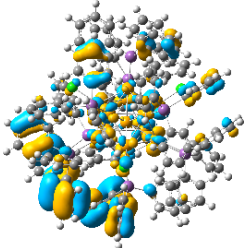
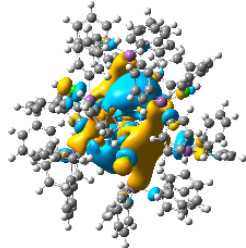
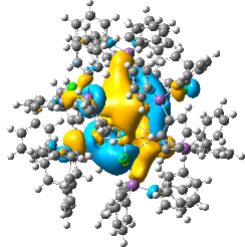
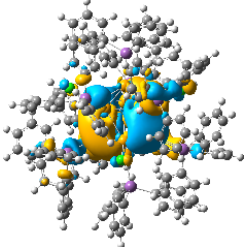
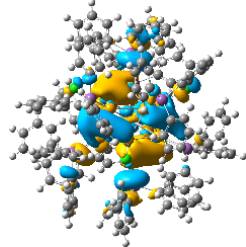
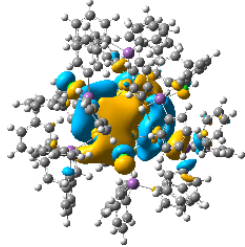
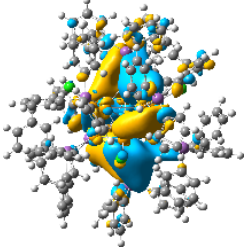
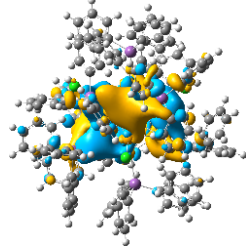
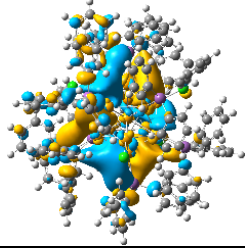
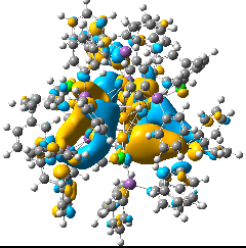
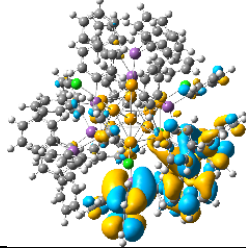
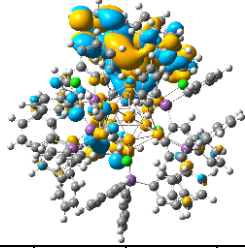
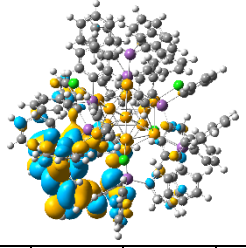
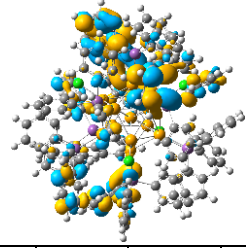
HOMO (-6.924 eV) Superatomic 1P orbital				HOMO-1 (-7.004 eV) Superatomic 1P orbital				HOMO-2 (-7.019 eV) Superatomic 1P orbital			
											
63	16	7	13	65	11	13	12	64	12	8	16
HOMO-3 (-7.708 eV)				HOMO-4 (-7.751 eV)				HOMO-5 (-7.808 eV)			
											
53	11	9	27	57	11	13	19	51	14	4	31
HOMO-6 (-7.977 eV)				HOMO-7 (-8.011 eV)				HOMO-8 (-8.033 eV)			
											
40	5	26	30	42	5	30	22	43	2	43	12
HOMO-9 (-8.058 eV)				HOMO-10 (-8.096 eV)				HOMO-29 (-8.533 eV)			
											
45	5	26	24	51	4	19	26	7	0	11	82

HOMO-33 (-8.570 eV)	HOMO-53 (-8.853 eV)	LUMO (-3.603 eV)
		
37 1 18 44	9 2 3 87	74 12 3 11
LUMO+1 (-3.535 eV)	LUMO+2 (-3.473 eV)	LUMO+3 (-3.410 eV)
		
74 11 6 9	68 16 1 15	70 13 3 14
LUMO+4 (-3.369 eV)	LUMO+5 (-2.508 eV)	LUMO+6 (2.447 eV)
		
73 12 3 12	48 17 0 35	41 16 1 42
LUMO+7 (-2.361 eV)	LUMO+16 (-2.929 eV)	LUMO+22 (-1.798 eV)
		
47 16 1 36	21 9 1 69	4 4 0 92

Note: The isovalue and density were set to 0.015 and 0.0004, respectively. The four numbers (rounded to the nearest integers) below each orbital are the contribution ratios (%) for Au, As, Cl and C elements, respectively.

Table S5. Selected orbitals of $\text{Au}_{13}\text{Sb}_8$ and elemental contribution ratios (%).

HOMO (-6.899 eV) Superatomic 1P orbital 				HOMO-1 (-7.043 eV) Superatomic 1P orbital 				HOMO-2 (-7.098 eV) Superatomic 1P orbital 			
61	17	9	13	63	12	15	11	63	11	16	11
HOMO-3 (-7.782 eV) 				HOMO-4 (-7.806 eV) 				HOMO-5 (-7.880 eV) 			
55	10	13	22	56	10	14	20	52	13	8	27
HOMO-6 (-8.012 eV) 				HOMO-7 (-8.018 eV) 				HOMO-8 (-8.047 eV) 			
33	3	43	21	37	2	52	9	39	4	36	21
HOMO-9 (-8.068 eV) 				HOMO-10 (-8.107 eV) 				HOMO-12 (-8.184 eV) 			
37	3	43	18	45	4	26	25	34	3	41	23
HOMO-23 (-8.417 eV) 				HOMO-33 (-8.537 eV) 				HOMO-36 (-8.556 eV) 			
9	1	13	77	1	0	1	97	7	0	8	85

HOMO-52 (-8.727 eV)				HOMO-61 (-8.845 eV)				LUMO (-3.806 eV)			
											
4	1	0	95	15	1	1	83	69	17	4	10
LUMO+1 (-3.692 eV)				LUMO+2 (-3.591 eV)				LUMO+3 (-3.573 eV)			
											
67	16	6	10	67	18	3	13	65	19	2	14
LUMO+4 (-3.510 eV)				LUMO+5 (-2.763 eV)				LUMO+6 (-2.696 eV)			
											
69	16	6	9	47	29	1	24	45	28	1	26
LUMO+7 (-2.582 eV)				LUMO+8 (-2.389 eV)				LUMO+11 (-2.198 eV)			
											
43	28	1	28	45	26	1	29	4	21	0	75
LUMO+13 (-2.117 eV)				LUMO+15 (-2.005 eV)				LUMO+17 (-1.949 eV)			
											
2	20	0	78	5	5	0	90	8	10	0	81

Note: The isovalue and density were set to 0.015 and 0.0004, respectively. The four numbers (rounded to the nearest integers) below each orbital are the contribution ratios (%) for Au, Sb, Cl and C elements, respectively.

Table S6. Selected excited states, energy, oscillator strength, and the most probable transitions of **Au₁₃As₈** from TD-DFT calculations.

State	Energy (nm)	Energy (ev)	Oscillator strength (a.u.)	Most probable transitions	Weight of Transition	Nature of major transitions
<i>Transitions contributing to the long-wavelength tail of the peak at 417 nm</i>						
1	494.92	2.5051	0.0094	HOMO→LUMO	0.82	MMCT (or superatomically metal-centered)
3	481.67	2.5741	0.0052	HOMO→LUMO+1	0.72	
6	463.89	2.6727	0.0077	HOMO→LUMO+2	0.40	
				HOMO-2→LUMO+2	0.32	
8	459.27	2.6996	0.0143	HOMO→LUMO+2	0.33	
				HOMO-1→LUMO+1	0.29	
11	448.64	2.7635	0.0091	HOMO-2→LUMO+3	0.50	
				HOMO-1→LUMO+4	0.27	
12	442.07	2.8046	0.0042	HOMO-1→LUMO+3	0.48	
				HOMO-2→LUMO+4	0.47	
<i>Transitions contributing to the absorption peak at 417 nm</i>						
13	420.78	2.9466	0.3186	HOMO-2→LUMO+2	0.37	MMCT (or superatomically metal-centered)
				HOMO-1→LUMO+1	0.15	
				HOMO-1→LUMO+4	0.14	
				HOMO→LUMO	0.10	
14	417.55	2.9694	0.1182	HOMO-2→LUMO+4	0.44	
				HOMO-1→LUMO+3	0.29	
15	415.87	2.9813	0.2156	HOMO-1→LUMO+4	0.37	
				HOMO-2→LUMO+3	0.24	
				HOMO→LUMO+2	0.12	
				HOMO-2→LUMO	0.09	
<i>Transitions contributing to the absorption peak at 335 nm</i>						
21	355.49	3.4877	0.0709	HOMO-4→LUMO+1	0.28	LMCT
				HOMO-3→LUMO+3	0.29	
				HOMO-3→LUMO+2	0.21	
23	351.11	3.5312	0.0784	HOMO-4→LUMO+2	0.80	
24	346.72	3.5759	0.0904	HOMO-3→LUMO+3	0.34	
				HOMO-4→LUMO+4	0.19	
27	342.50	3.6199	0.1547	HOMO-6→LUMO	0.49	
				HOMO-3→LUMO+4	0.13	
29	341.49	3.6307	0.1817	HOMO-3→LUMO+4	0.35	
				HOMO-8→LUMO	0.25	
30	340.15	3.6450	0.0954	HOMO-7→LUMO+1	0.40	
				HOMO-8→LUMO	0.14	
32	339.63	3.6506	0.1384	HOMO-9→LUMO	0.44	

				HOMO-6→LUMO+1	0.34	
33	338.31	3.6649	0.4281	HOMO-5→LUMO+2	0.41	
				HOMO-8→LUMO	0.17	
38	334.58	3.7057	0.0992	HOMO-5→LUMO+4	0.41	
				HOMO-10→LUMO	0.23	
42	329.79	3.7595	0.1489	HOMO-10→LUMO	0.32	
				HOMO-5→LUMO+4	0.25	
53	322.52	3.8442	0.1199	HOMO→LUMO+7	0.17	
				HOMO-8→LUMO+3	0.12	
				HOMO-6→LUMO+3	0.12	
				HOMO-7→LUMO+4	0.09	
61	317.96	3.8994	0.0880	HOMO-7→LUMO+4	0.28	
				HOMO→LUMO+7	0.13	
				HOMO-10→LUMO+4	0.13	
<i>Transitions contributing to the featureless absorptions below 300 nm</i>						
103	291.68	4.2507	0.0197	HOMO→LUMO+12	0.61	MLCT and LMCT
				HOMO-1→LUMO+8	0.25	
110	289.88	4.2770	0.0195	HOMO→LUMO+13	0.36	
123	287.81	4.3078	0.0221	HOMO-33→LUMO+2	0.32	
				HOMO-23→LUMO+2	0.12	
134	285.68	4.3399	0.0212	HOMO-14→LUMO+4	0.24	
150	282.63	4.3867	0.0229	HOMO-16→LUMO+3	0.21	
154	282.13	4.3946	0.0462	HOMO→LUMO+16	0.36	
165	280.54	4.4196	0.0172	HOMO-29→LUMO	0.46	
295	263.95	4.6973	0.0476	HOMO-4→LUMO+7	0.26	
				HOMO-1→LUMO+22	0.22	
298	263.63	4.7030	0.0233	HOMO-53→LUMO	0.46	

Table S7. Selected excited states, energy, oscillator strength, and the most probable transitions of $\text{Au}_{13}\text{Sb}_8$ from TD-DFT calculations.

State	Energy (nm)	Energy (ev)	Oscillator strength (a.u.)	Most probable transitions	Weight of Transition	Nature of major transitions
<i>Transitions contributing to the long-wavelength tail of the peak at 435 nm</i>						
1	535.77	2.3141	0.0221	HOMO→LUMO	0.89	MMCT (or superatomically metal-centered)
3	506.71	2.4469	0.0099	HOMO-1→LUMO	0.42	
				HOMO→LUMO+1	0.40	
5	493.58	2.5119	0.0104	HOMO→LUMO+2	0.64	
8	481.52	2.5748	0.0159	HOMO→LUMO+3	0.59	
10	464.16	2.6711	0.0252	HOMO-1→LUMO+2	0.40	
<i>Transitions contributing to the absorption peak at 435 nm</i>						
13	437.00	2.8372	0.3044	HOMO-1→LUMO+3	0.32	MMCT (or superatomically metal-centered)
				HOMO-2→LUMO+1	0.20	
14	431.04	2.8764	0.1246	HOMO-1→LUMO+4	0.40	
				HOMO-2→LUMO+2	0.24	
15	427.55	2.8998	0.1679	HOMO-2→LUMO+4	0.65	
<i>Transitions contributing to the absorption peak at 340 nm</i>						
19	371.31	3.3391	0.0494	HOMO-5→LUMO	0.44	LMCT
				HOMO-3→LUMO+1	0.31	
27	356.65	3.4764	0.0121	HOMO-4→LUMO+2	0.40	
				HOMO-6→LUMO	0.18	
30	354.33	3.4992	0.0536	HOMO-4→LUMO+3	0.20	
				HOMO-7→LUMO+1	0.09	
				HOMO-3→LUMO+3	0.08	
35	348.85	3.5540	0.1007	HOMO-1→LUMO+5	0.15	
				HOMO-9→LUMO+1	0.09	
				HOMO-8→LUMO+1	0.08	
37	347.90	3.5638	0.1039	HOMO-3→LUMO+4	0.26	
				HOMO-2→LUMO+5	0.10	
				HOMO-5→LUMO+2	0.08	
41	345.41	3.5894	0.2407	HOMO-9→LUMO+1	0.25	
				HOMO-3→LUMO+4	0.18	
42	344.55	3.5985	0.0789	HOMO-2→LUMO+5	0.42	
				HOMO→LUMO+7	0.14	
45	340.01	3.6465	0.0843	HOMO-10→LUMO+1	0.63	
46	339.29	3.6542	0.1510	HOMO-2→LUMO+6	0.23	
				HOMO-5→LUMO+4	0.22	
47	338.61	3.6615	0.1461	HOMO-6→LUMO+2	0.14	
				HOMO-7→LUMO+2	0.15	

				HOMO-5→LUMO+4	0.12	
				HOMO-2→LUMO+5	0.11	
48	337.92	3.6690	0.1185	HOMO-5→LUMO+4	0.30	
				HOMO-2→LUMO+6	0.28	
50	336.18	3.6880	0.2049	HOMO-7→LUMO+2	0.28	
				HOMO-7→LUMO+4	0.09	
51	335.56	3.6948	0.0734	HOMO-6→LUMO+2	0.26	
				HOMO-2→LUMO+6	0.16	
52	334.70	3.7043	0.0630	HOMO-7→LUMO+4	0.14	
				HOMO-7→LUMO+3	0.14	
				HOMO-6→LUMO+3	0.23	
55	332.86	3.7248	0.0680	HOMO-9→LUMO+2	0.19	
				HOMO-12→LUMO+1	0.18	
66	325.19	3.8127	0.0551	HOMO-2→LUMO+7	0.19	
				HOMO-8→LUMO+4	0.17	
87	310.31	3.9955	0.0572	HOMO-2→LUMO+8	0.47	
<i>Transitions contributing to the featureless absorptions below 300 nm</i>						
126	296.65	4.1795	0.0173	HOMO→LUMO+11	0.58	MLCT and LMCT
				HOMO→LUMO+10	0.17	
144	292.70	4.2359	0.0132	HOMO-33→LUMO	0.17	
152	290.93	4.2617	0.0186	HOMO→LUMO+13	0.74	
182	285.76	4.3387	0.0158	HOMO→LUMO+14	0.23	
				HOMO-4→LUMO+5	0.15	
196	284.25	4.3618	0.0139	HOMO-23→LUMO+3	0.09	
				HOMO-33→LUMO+1	0.09	
				HOMO→LUMO+15	0.34	
216	281.82	4.3994	0.0433	HOMO→LUMO+16	0.11	
				HOMO-1→LUMO+13	0.21	
220	281.35	4.4068	0.0201	HOMO→LUMO+15	0.15	
				HOMO-2→LUMO+12	0.56	
224	280.93	4.4134	0.0125	HOMO-1→LUMO+13	0.19	
				HOMO→LUMO+17	0.43	
236	279.58	4.4347	0.0106	HOMO-52→LUMO	0.14	
				HOMO-2→LUMO+13	0.49	
256	277.32	4.4708	0.0090	HOMO→LUMO+18	0.22	
				HOMO-3→LUMO+7	0.16	
286	274.00	4.5249	0.0095	HOMO-36→LUMO+3	0.10	
294	273.20	4.5383	0.0124	HOMO-61→LUMO	0.18	

Table S8. Cartesian coordinates of optimized **Au₁₃As₈** and **Au₁₃Sb₈**.

Au₁₃As₈				Au₁₃Sb₈			
Au	0	0.000002	-0.14113	Au	0.348507	-2.37532	-1.67019
Au	-0.26529	-2.38504	-1.6918	Au	-2.21613	-1.75561	-0.25677
Au	2.277817	-1.73199	-0.21778	Au	-1.52999	-0.17479	2.183317
Au	-2.59271	-1.26194	-0.11724	Au	0.222926	-2.35717	1.295395
Au	1.501261	-0.16275	2.248053	Au	-1.38125	-0.17142	-2.59268
Au	-0.21258	-2.38079	1.28767	Au	0.008135	-0.00985	-0.16791
Au	-1.50141	0.162698	2.247964	Sb	4.880869	-2.52127	0.00123
Au	2.592694	1.26194	-0.11705	Sb	0.76913	-4.41832	-3.24795
Au	0.265388	2.38508	-1.69172	Sb	-4.19632	-3.45901	-0.5508
Au	-1.48591	0.109635	-2.52809	Sb	-4.88299	2.465266	-0.24461
Au	1.486055	-0.10958	-2.528	Sb	4.159981	3.514564	-0.50837
Au	-2.27782	1.731988	-0.21787	Sb	-2.83011	-0.38402	4.451506
Au	0.212484	2.380751	1.287751	Au	2.596464	-1.20834	-0.08217
As	4.177469	-3.30164	-0.45174	Au	-2.57421	1.200076	-0.2015
As	-0.5628	-4.30534	-3.19568	Au	-0.27732	2.346443	-1.70783
As	0.563069	4.305394	-3.19555	Au	2.217136	1.778851	-0.19334
As	-4.17745	3.301638	-0.45194	Au	1.454237	0.200854	2.225362
As	-4.7472	-2.49717	-0.1011	Au	1.542173	0.142956	-2.50565
As	2.723854	-0.32917	4.384746	Au	-0.28098	2.367055	1.250142
As	-2.72415	0.329068	4.384577	Sb	-0.62189	4.399848	-3.27562
As	4.747161	2.4972	-0.10081	Sb	2.650725	0.460881	4.54003
Cl	2.766894	0.037252	-4.5645	Cl	0.277208	-4.37477	2.733061
Cl	-2.76657	-0.03723	-4.5647	Cl	-2.74354	-0.07014	-4.63509
Cl	0.323248	4.443927	2.571334	Cl	3.163847	0.276873	-4.34696
C	0.498579	-6.09069	-1.2204	Cl	-0.38351	4.437514	2.602639
C	0.396281	-5.87044	-2.59656	C	6.276489	-2.10155	1.55912
C	1.120064	-7.24211	-0.74486	C	6.239685	-2.83594	2.760302
C	1.558546	-7.9447	-3.00956	C	7.181893	-2.58618	3.76888
C	1.64611	-8.17125	-1.63885	C	8.169442	-1.60763	3.584959
C	0.936568	-6.79601	-3.49071	C	8.204199	-0.86719	2.393815
H	0.098925	-5.36699	-0.51552	C	7.256381	-1.10308	1.387459
H	1.200927	-7.40206	0.324314	C	6.179148	-2.42232	-1.68186
H	2.130462	-9.06791	-1.2667	C	7.531755	-2.80817	-1.57603
H	1.975952	-8.66169	-3.7086	C	8.368428	-2.75536	-2.69926
H	0.8837	-6.61952	-4.55903	C	7.865212	-2.30905	-3.93231
C	-5.96135	-2.29552	1.401235	C	6.523923	-1.91543	-4.03799
C	-5.88537	-3.16843	2.488714	C	5.679972	-1.97376	-2.91847
C	-6.80595	-3.07227	3.528451	C	4.603703	-4.60754	0.332056
C	-7.88295	-1.23356	2.405915	C	3.352415	-5.07116	0.778047
C	-6.95067	-1.31025	1.375194	C	3.151759	-6.43778	1.029698
C	-7.81636	-2.11513	3.481627	C	4.199073	-7.34813	0.833456
H	-8.5494	-2.05882	4.279578	C	5.451349	-6.89057	0.389673
H	-6.73752	-3.75553	4.367282	C	5.655044	-5.52659	0.139924
H	-7.01927	-0.61811	0.543414	C	2.744054	-4.86762	-3.91096
H	-8.66627	-0.48512	2.357922	C	3.606163	-5.64638	-3.11452
H	-5.12218	-3.93755	2.520531	C	4.886435	-5.97655	-3.58169

C	4.218387	-4.75803	0.813895	C	5.316573	-5.52779	-4.83855
C	3.084674	-5.01023	1.585067	C	4.465279	-4.74156	-5.62857
C	3.075279	-6.06986	2.489744	C	3.183843	-4.40857	-5.16798
C	5.350409	-5.5683	0.959179	C	0.199998	-6.31565	-2.47685
C	4.198131	-6.88083	2.625067	C	-0.59182	-6.38089	-1.31538
C	5.336131	-6.62794	1.860427	C	-0.98787	-7.62288	-0.79825
H	6.245939	-5.36874	0.380268	C	-0.59096	-8.807	-1.43554
H	6.214923	-7.25541	1.965866	C	0.212066	-8.74953	-2.58541
H	4.190965	-7.70817	3.327264	C	0.610495	-7.50987	-3.10371
H	2.182883	-6.24608	3.080618	C	-0.17885	-4.22831	-5.14161
H	2.200799	-4.38779	1.494463	C	-0.46232	-5.35283	-5.94096
C	3.883897	-3.33709	-3.30636	C	-0.99856	-5.1834	-7.22446
C	4.602959	-5.45245	-2.3851	C	-1.25891	-3.89362	-7.71614
C	4.701124	-5.97338	-3.67154	C	-0.99302	-2.77307	-6.91716
C	3.994018	-3.86116	-4.59204	C	-0.45301	-2.93832	-5.63249
C	4.406439	-5.17758	-4.77547	C	-4.19839	-4.38944	-2.46388
C	4.203941	-4.12792	-2.20027	C	-3.91021	-3.60427	-3.59779
H	4.82844	-6.08286	-1.5331	C	-3.98093	-4.17033	-4.87897
H	3.548501	-2.31118	-3.18321	C	-4.32571	-5.51997	-5.03457
H	4.489341	-5.58549	-5.77728	C	-4.59258	-6.30979	-3.90606
H	5.009506	-7.00428	-3.80918	C	-4.53058	-5.7489	-2.62278
H	3.743049	-3.23616	-5.44102	C	-6.22717	-2.80227	-0.46447
C	-4.46286	-4.41068	-0.0633	C	-6.85115	-2.29499	-1.62134
C	-5.42267	-5.31196	-0.52722	C	-8.19493	-1.89635	-1.58111
C	-3.11407	-6.2577	0.718447	C	-8.92834	-2.00926	-0.39015
C	-3.30369	-4.88778	0.549493	C	-8.30725	-2.5033	0.766437
C	-4.07825	-7.15342	0.267388	C	-6.95874	-2.88897	0.735664
C	-5.22716	-6.67896	-0.36148	C	-4.25065	-5.09427	0.806999
H	-2.54199	-4.2031	0.908202	C	-3.1341	-5.34255	1.627481
H	-3.93403	-8.22058	0.39985	C	-3.13315	-6.43619	2.507191
H	-2.21031	-6.6065	1.205588	C	-4.24665	-7.28593	2.574553
H	-5.97582	-7.37479	-0.72505	C	-5.36674	-7.03814	1.764091
H	-6.31612	-4.95658	-1.0266	C	-5.37178	-5.9467	0.884334
C	1.679981	-1.17765	5.775857	C	-6.17004	2.090442	-1.89547
C	0.324847	-2.61578	7.743854	C	-5.65935	1.422874	-3.02352
C	0.880744	-2.26721	5.421578	C	-6.49036	1.160993	-4.12338
C	1.777436	-0.79387	7.113908	C	-7.83218	1.566995	-4.10504
C	0.213729	-2.98952	6.407991	C	-8.34749	2.230326	-2.97923
C	1.098288	-1.5121	8.093161	C	-7.52288	2.488214	-1.87568
H	-0.39721	-3.83707	6.120714	C	-4.65899	4.578423	-0.1208
H	-0.19617	-3.17915	8.510747	C	-3.48712	5.096315	0.462616
H	2.371235	0.066891	7.397264	C	-3.34548	6.479405	0.653498
H	1.177649	-1.2083	9.131598	C	-4.37065	7.350807	0.260524
H	0.772146	-2.56807	4.383123	C	-5.53624	6.838929	-0.33164
C	4.335116	-1.41244	4.437293	C	-5.68178	5.458424	-0.52415
C	5.594185	-0.82416	4.306856	C	-6.28603	2.195485	1.343769
C	5.384809	-3.57274	4.714623	C	-7.23833	1.159617	1.277231
C	6.641317	-2.97778	4.627326	C	-8.21318	1.034055	2.277392
C	4.235648	-2.79323	4.626647	C	-8.2343	1.925583	3.360244

C	6.741554	-1.60541	4.418591	C	-7.27026	2.941422	3.445223
H	3.264891	-3.26549	4.725331	C	-6.3011	3.079307	2.440648
H	5.294439	-4.64348	4.858764	C	0.174215	6.204241	-2.47938
H	7.536978	-3.58291	4.720935	C	0.388167	6.279705	-1.08936
H	7.714171	-1.13126	4.346144	C	0.87064	7.463754	-0.51206
H	5.692146	0.242466	4.139572	C	1.141466	8.578301	-1.31901
C	-4.19698	-1.43287	6.186723	C	0.936472	8.505649	-2.70589
C	-3.30586	-1.36189	5.109628	C	0.457304	7.322839	-3.28665
C	-3.17638	-3.77483	5.071131	C	-2.60185	4.988085	-3.78636
C	-2.80293	-2.53701	4.551882	C	-3.40038	4.10117	-4.53699
C	-4.0514	-3.84186	6.151086	C	-4.67578	4.498647	-4.96124
C	-4.56334	-2.67012	6.706584	C	-5.16127	5.775608	-4.64082
H	-4.61505	-0.52728	6.613494	C	-4.37345	6.653136	-3.88292
H	-5.24977	-2.71839	7.545381	C	-3.09729	6.261368	-3.45134
H	-4.33834	-4.80518	6.560101	C	0.145368	4.172226	-5.24391
H	-2.77009	-4.67572	4.623823	C	1.008917	3.102592	-5.53859
H	-2.1141	-2.50147	3.714034	C	1.474276	2.913929	-6.8482
C	5.91783	2.134476	-1.59353	C	1.086913	3.795619	-7.86645
C	7.251371	2.559526	-1.60036	C	0.221233	4.863168	-7.57762
C	5.411597	1.433735	-2.68665	C	-0.25616	5.048061	-6.2733
C	8.057623	2.302264	-2.70426	C	4.345318	5.055921	0.941014
C	6.223151	1.17219	-3.78873	C	3.357954	5.176578	1.937432
C	7.543926	1.610847	-3.80073	C	3.430733	6.212525	2.880937
H	5.804836	0.628929	-4.62907	C	4.489659	7.130015	2.839884
H	8.176285	1.411517	-4.65981	C	5.476357	7.01642	1.8474
H	9.089129	2.638682	-2.70599	C	5.404826	5.987094	0.898999
H	7.669769	3.072707	-0.74115	C	6.119777	2.667231	-0.62227
H	4.3846	1.0847	-2.69785	C	6.372322	1.70499	-1.62176
C	-0.49898	6.090641	-1.22053	C	7.664825	1.189364	-1.79534
C	-0.39629	5.870419	-2.59666	C	8.713402	1.622058	-0.96912
C	-0.9364	6.795964	-3.49095	C	8.46087	2.557255	0.045359
C	-1.12068	7.242014	-0.74514	C	7.16869	3.07633	0.222591
C	-1.5586	7.944596	-3.00996	C	4.142307	4.62011	-2.3342
C	-1.64656	8.171125	-1.63927	C	4.174084	6.027584	-2.33373
H	-0.09947	5.366961	-0.51555	C	4.241424	6.729038	-3.54616
H	-0.88323	6.61949	-4.55925	C	4.273466	6.034034	-4.76312
H	-1.97587	8.661561	-3.7091	C	4.217024	4.633069	-4.76699
H	-2.13108	9.067742	-1.26724	C	4.145253	3.924444	-3.5595
H	-1.20185	7.401946	0.324009	C	1.500358	1.33523	6.10037
C	-5.33646	6.627724	1.860365	C	0.695359	2.453786	5.805349
C	-5.3506	5.568176	0.959005	C	0.009465	3.113218	6.836044
C	-4.21855	4.757923	0.813814	C	0.117038	2.659627	8.158829
C	-4.19858	6.880529	2.625213	C	0.903461	1.535478	8.451069
C	-3.07571	6.069573	2.489984	C	1.593041	0.871506	7.426266
C	-3.08496	5.010035	1.585192	C	4.380008	1.703719	4.648509
H	-2.20108	4.387594	1.49467	C	4.413316	2.817932	5.509006
H	-2.18341	6.245715	3.081024	C	5.565352	3.614285	5.587688
H	-4.19152	7.707787	3.3275	C	6.689981	3.304815	4.809961
H	-6.21527	7.255183	1.965732	C	6.659146	2.198005	3.948995

H	-6.24604	5.368677	0.379935	C	5.509116	1.401557	3.862704
C	-2.67035	-6.31445	-3.3495	C	3.397719	-1.34161	5.385868
C	-2.3578	-4.96286	-3.49106	C	4.37464	-1.31292	6.401256
C	-3.93398	-6.7748	-3.71279	C	4.844638	-2.51064	6.958324
C	-3.3145	-4.06866	-3.97965	C	4.352702	-3.74291	6.497736
C	-4.88255	-5.88942	-4.2133	C	3.391308	-3.77548	5.476967
C	-4.57418	-4.53653	-4.33968	C	2.912344	-2.57879	4.922501
H	-3.07564	-3.0154	-4.10149	C	-3.5647	1.443319	5.250061
H	-1.9311	-7.01034	-2.96914	C	-3.05892	2.654868	4.742343
H	-5.31289	-3.84008	-4.71994	C	-3.50433	3.879244	5.262452
H	-5.86302	-6.25116	-4.50492	C	-4.45454	3.901209	6.293417
H	-4.17102	-7.82824	-3.60831	C	-4.96454	2.695606	6.801972
C	-3.99371	3.861512	-4.59219	C	-4.52519	1.470072	6.282066
C	-3.8837	3.337323	-3.30655	C	-1.7501	-1.27534	6.055396
C	-4.60263	5.45266	-2.38514	C	-0.88348	-2.35099	5.780101
C	-4.20373	4.128079	-2.2004	C	-0.24849	-3.02588	6.833754
C	-4.406	5.177988	-4.77552	C	-0.46797	-2.62952	8.160323
C	-4.70067	5.973719	-3.67154	C	-1.31609	-1.54609	8.43457
H	-4.48881	5.585992	-5.7773	C	-1.95504	-0.86807	7.387269
H	-3.74276	3.23656	-5.4412	C	-4.57783	-1.60992	4.528098
H	-5.00895	7.004658	-3.8091	C	-4.44784	-2.98854	4.789563
H	-4.8281	6.083016	-1.5331	C	-5.58635	-3.80178	4.877546
H	-3.54841	2.311362	-3.18347	C	-6.86409	-3.24487	4.715949
Cl	-0.32346	-4.44399	2.571199	C	-6.99716	-1.87539	4.444832
C	0.671451	-2.8221	-5.34343	C	-5.86018	-1.06021	4.339471
C	-0.04249	-3.97456	-5.02437	H	4.264446	7.813668	-3.53512
C	-0.43621	-4.85291	-6.03995	H	4.329353	6.577845	-5.70029
C	1.006505	-2.55201	-6.66818	H	4.137253	6.584548	-1.40399
C	0.63511	-3.4382	-7.67415	H	4.07982	2.840668	-3.59846
C	-0.08627	-4.58857	-7.35943	H	4.217643	4.088138	-5.70393
H	1.548531	-1.64061	-6.89531	H	-0.09246	5.539342	-8.36619
H	0.892859	-3.22731	-8.70675	H	-0.95928	5.852303	-6.0763
H	-1.03575	-5.72731	-5.80831	H	2.127844	2.07431	-7.058
H	0.958728	-2.11577	-4.57294	H	1.444365	3.647072	-8.88025
H	-0.39202	-5.27274	-8.1439	H	-2.50051	6.95006	-2.86194
C	-1.68035	1.177436	5.775802	H	-4.74669	7.638668	-3.62513
C	-1.77791	0.793597	7.113829	H	-6.1467	6.081103	-4.97695
C	-0.32529	2.615417	7.743964	H	-5.28538	3.811673	-5.53747
C	-0.88104	2.26698	5.421632	H	-3.04052	3.110741	-4.80313
C	-0.21406	2.989214	6.408127	H	0.18077	5.428629	-0.44624
C	-1.0988	1.511759	8.093164	H	1.033005	7.506149	0.559443
H	0.195701	3.178732	8.51092	H	1.511815	9.49545	-0.87256
H	0.396941	3.836746	6.120933	H	1.149204	9.364936	-3.33352
H	-2.37177	-0.06715	7.397103	H	0.318962	7.279953	-4.36231
H	-1.17825	1.207909	9.131581	H	2.519329	4.488258	1.983576
H	-0.77235	2.567892	4.383199	H	2.656658	6.295351	3.635913
C	4.196455	1.432735	6.187107	H	4.545218	7.930288	3.570652
C	3.305443	1.361776	5.109925	H	6.294096	7.728581	1.807169
C	2.802508	2.536902	4.5522	H	6.168458	5.926029	0.12942

C	4.562712	2.669975	6.707068	H	5.579332	1.349526	-2.27408
C	3.175851	3.774705	5.071548	H	7.846739	0.455264	-2.57235
C	4.050771	3.841722	6.151586	H	9.715374	1.231998	-1.11484
H	4.614518	0.52714	6.613872	H	9.26762	2.893704	0.689176
H	5.249069	2.718231	7.545932	H	6.991203	3.794415	1.015996
H	4.33764	4.805031	6.560679	H	-2.67981	4.443644	0.783272
H	2.769567	4.675607	4.624254	H	-2.43936	6.859561	1.111758
H	2.113753	2.501377	3.714291	H	-4.26357	8.419935	0.412305
C	-0.67041	2.821988	-5.34363	H	-6.32963	7.511161	-0.64172
C	0.437091	4.852992	-6.03984	H	-6.58512	5.082984	-0.99357
C	0.087541	4.588618	-7.35941	H	-4.62447	1.096674	-3.0699
C	-0.63356	3.438128	-7.67433	H	-6.07776	0.643229	-4.9826
C	-1.00507	2.551863	-6.66848	H	-8.47346	1.367325	-4.95761
C	0.043258	3.974565	-5.02437	H	-9.3867	2.542195	-2.95827
H	1.036429	5.727492	-5.80803	H	-7.94512	2.977526	-1.00298
H	0.393378	5.272848	-8.14379	H	-5.57781	3.885335	2.512447
H	-0.89101	3.227207	-8.70701	H	-7.27435	3.630029	4.283063
H	-1.54687	1.640374	-6.89576	H	-8.99499	1.8336	4.128711
H	-0.95775	2.115593	-4.57323	H	-8.95501	0.246442	2.200789
C	-6.66106	2.59278	0.880292	H	-7.2456	0.460981	0.4465
C	-6.62314	2.116996	-1.48592	H	-4.9412	0.547427	6.675835
C	-7.93542	1.658665	-1.41432	H	-5.70055	2.708241	7.599289
C	-7.98159	2.156335	0.941613	H	-4.79596	4.848353	6.698719
C	-5.98402	2.598196	-0.34098	H	-3.10247	4.802145	4.85826
C	-8.62296	1.692173	-0.20367	H	-2.31593	2.66607	3.950278
H	-8.507	2.187104	1.88998	H	0.592693	2.825688	4.788678
H	-9.65404	1.358089	-0.15474	H	-0.60651	3.973229	6.599503
H	-8.42033	1.284948	-2.30906	H	-0.41257	3.174148	8.953877
H	-6.17598	2.948149	1.78256	H	0.981048	1.174135	9.471229
H	-6.10983	2.1148	-2.44073	H	2.186686	-0.00469	7.666304
C	-6.22316	-1.17184	-3.78893	H	3.553073	3.068988	6.12087
C	-5.41162	-1.43346	-2.68685	H	5.581409	4.470545	6.25372
C	-5.91783	-2.13438	-1.59383	H	7.5812	3.920447	4.874365
C	-7.25134	-2.55953	-1.60076	H	7.524468	1.947957	3.345699
C	-8.05758	-2.30219	-2.70466	H	5.512426	0.547503	3.192003
C	-7.5439	-1.6106	-3.80102	H	-0.69412	-2.68131	4.761607
H	-7.66973	-3.07285	-0.74163	H	0.413764	-3.85446	6.610538
H	-4.38465	-1.08434	-2.69797	H	0.021057	-3.15658	8.972978
H	-5.80485	-0.62844	-4.62918	H	-1.48174	-1.22903	9.459048
H	-9.08906	-2.63869	-2.70647	H	-2.59593	-0.0233	7.616977
H	-8.17624	-1.41121	-4.6601	H	-5.47368	-4.86157	5.078691
C	6.660925	-2.59294	0.880869	H	-7.74496	-3.87247	4.803891
C	7.981448	-2.15651	0.942396	H	-7.98063	-1.43484	4.320324
C	8.622956	-1.69223	-0.20276	H	-5.98948	-0.00407	4.126792
C	7.935565	-1.65858	-1.41348	H	-3.47086	-3.43607	4.94295
C	6.62329	-2.1169	-1.48529	H	4.718322	-4.66873	6.930309
C	5.98403	-2.59822	-0.34049	H	5.591465	-2.48157	7.745129
H	9.654031	-1.35815	-0.15367	H	4.780818	-0.36788	6.749857
H	8.506746	-2.18739	1.890822	H	2.164021	-2.63282	4.137094

H	6.175736	-2.94841	1.783041	H	3.008281	-4.72042	5.106526
H	8.420578	-1.28477	-2.30813	H	5.494439	-3.60973	2.914337
H	6.110092	-2.1146	-2.44016	H	7.142259	-3.15651	4.690147
C	4.462782	4.410709	-0.06299	H	8.903345	-1.42301	4.362341
C	5.422544	5.312019	-0.52694	H	8.969386	-0.11332	2.239845
C	5.226989	6.679007	-0.36123	H	7.30303	-0.52027	0.472856
C	4.078071	7.153441	0.267649	H	4.650502	-1.64868	-3.0322
C	3.113925	6.257689	0.718739	H	6.123473	-1.55783	-4.97994
C	3.303597	4.887777	0.549804	H	8.515608	-2.26476	-4.79989
H	3.933813	8.220599	0.400094	H	9.407505	-3.0556	-2.61045
H	2.210161	6.606465	1.205887	H	7.94588	-3.1275	-0.62425
H	5.97561	7.374867	-0.72482	H	3.289636	-6.01138	-2.14214
H	2.541921	4.203075	0.908528	H	5.540438	-6.58099	-2.96281
H	6.316	4.956658	-1.02633	H	6.30794	-5.78414	-5.19707
C	-5.38502	3.572712	4.714398	H	4.793434	-4.38903	-6.60064
C	-6.64154	2.977781	4.62709	H	2.535048	-3.80665	-5.79623
C	-6.74181	1.605417	4.418349	H	-0.2792	-6.35717	-5.57338
C	-5.59447	0.824142	4.306617	H	-1.21027	-6.05328	-7.83774
C	-4.33538	1.412384	4.437069	H	-1.67065	-3.76547	-8.71192
C	-4.23588	2.793172	4.626432	H	-1.2106	-1.77306	-7.27437
H	-3.26511	3.265405	4.725133	H	-0.26723	-2.05586	-5.02824
H	-5.69245	-0.24249	4.139335	H	-3.61923	-2.56053	-3.5102
H	-5.29462	4.643448	4.858547	H	-3.74986	-3.55726	-5.74212
H	-7.53719	3.582934	4.720696	H	-4.37339	-5.95594	-6.02682
H	-7.71444	1.131292	4.345895	H	-4.84527	-7.35866	-4.02195
C	4.883026	5.889757	-4.21187	H	-4.72834	-6.37784	-1.76096
C	4.574766	4.536846	-4.33838	H	-6.30977	-2.22254	-2.55941
C	3.314995	4.068905	-3.97876	H	-6.49797	-3.26603	1.64314
C	2.358094	4.963044	-3.49047	H	-8.86805	-2.59782	1.690565
C	2.67052	6.314649	-3.34877	H	-9.97325	-1.71764	-0.36683
C	3.934249	6.775077	-3.71165	H	-8.66486	-1.50684	-2.47749
H	4.171201	7.828525	-3.60708	H	-6.25084	-5.76208	0.274068
H	1.93112	7.010499	-2.96862	H	-6.23208	-7.69082	1.815779
H	5.863571	6.251554	-4.50317	H	-4.24529	-8.13257	3.253494
H	5.313645	3.840448	-4.7184	H	-2.26287	-6.60867	3.131091
H	3.076243	3.015628	-4.10067	H	-2.2601	-4.69766	1.604515
C	5.961294	2.295547	1.401541	H	1.322656	2.400772	-4.77262
C	5.885252	3.168404	2.489062	H	2.524482	-4.38847	0.943984
C	6.950703	1.310369	1.375447	H	6.62787	-5.19341	-0.20721
C	6.80584	3.072272	3.528791	H	6.26581	-7.5925	0.24219
H	5.122003	3.93746	2.520914	H	2.181707	-6.77183	1.379619
C	7.88299	1.233708	2.406159	H	4.044799	-8.4047	1.025893
H	7.019363	0.618281	0.543627	H	1.255715	-7.4832	-3.97684
C	7.816338	2.115218	3.481915	H	0.531395	-9.66445	-3.07347
H	6.737364	3.755481	4.367653	H	-0.89734	-9.76806	-1.03562
H	8.666384	0.485338	2.358123	H	-1.59694	-7.65952	0.098217
H	8.549387	2.058934	4.279858	H	-0.88877	-5.47215	-0.79977

Table S9. Natural Population charges for $\text{Au}_{13}\text{As}_8$ and $\text{Au}_{13}\text{Sb}_8$.

$\text{Au}_{13}\text{As}_8$			$\text{Au}_{13}\text{Sb}_8$		
Atom		Natural Charge	Atom		Natural Charge
central	Au1	-2.12338	central	Au6	-2.11650
As-bonded	Au2	0.11242	Sb-bonded	Au1	-0.02581
	Au3	0.12980		Au2	0.00244
	Au4	0.12709		Au3	-0.00304
	Au5	0.11865		Au13	0.00312
	Au7	0.11865		Au14	-0.00312
	Au8	0.12710		Au15	-0.02604
	Au9	0.11242		Au16	-0.00512
	Au12	0.12980		Au17	-0.00512
	<i>Sub-total</i>	<i>0.97593</i>		<i>Sub-total</i>	<i>-0.06269</i>
Cl-bonded	Au6	0.15277	Cl-bonded	Au4	0.17111
	Au10	0.17016		Au5	0.20298
	Au11	0.17015		Au18	0.19987
	Au13	0.15277		Au19	0.17327
		<i>Sub-total</i>		<i>0.64585</i>	
Total for all Au		-0.50160	Total for all Au		-1.43196
	As14	1.11853		Sb7	1.60701
	As15	1.13783		Sb8	1.63460
	As16	1.13783		Sb9	1.60733
	As17	1.11853		Sb10	1.61063
	As18	1.11877		Sb11	1.61069
	As19	1.12219		Sb12	1.61920
	As20	1.12219		Sb20	1.64111
	As21	1.11877		Sb21	1.61968
	Total for As	8.99464		Total for Sb	12.95025
	Cl22	-0.54213		Cl22	-0.57386
	Cl23	-0.54213		Cl23	-0.54859
	Cl24	-0.57071		Cl24	-0.54959
	Cl168	-0.57071		Cl25	-0.56982
	Total for Cl	-2.22568		Total for Cl	-2.24186
	Total for C	-36.56340		Total for C	-38.96133
	Total for H	31.29594		Total for H	31.16375
	Total for all	1		Total for all	1

Table S10. Mulliken charges for $\text{Au}_{13}\text{As}_8$ and $\text{Au}_{13}\text{Sb}_8$.

$\text{Au}_{13}\text{As}_8$			$\text{Au}_{13}\text{Sb}_8$		
Atom		Mulliken Charge	Atom		Mulliken Charge
central	Au1	4.11665	central	Au6	5.07580
As-bonded	Au2	-0.30978	Sb-bonded	Au1	-0.41133
	Au3	-0.43702		Au2	-0.56941
	Au4	-0.46671		Au3	-0.51546
	Au5	-0.29256		Au13	-0.45585
	Au7	-0.29263		Au14	-0.50828
	Au8	-0.46664		Au15	-0.43740
	Au9	-0.30970		Au16	-0.56803
	Au12	-0.43695		Au17	-0.45241
	<i>Sub-total</i>	<i>-3.01199</i>		<i>Sub-total</i>	<i>-3.91817</i>
Cl-bonded	Au6	-0.79378	Cl-bonded	Au4	-0.97794
	Au10	-0.73396		Au5	-0.72849
	Au11	-0.73386		Au18	-0.79436
	Au13	-0.79384		Au19	-0.92597
		<i>Sub-total</i>		<i>-3.05544</i>	
Total for all Au		-1.95078	Total for all Au		-2.26913
	As14	0.410090		Sb7	0.887604
	As15	0.415329		Sb8	0.907113
	As16	0.415339		Sb9	0.872512
	As17	0.410082		Sb10	0.891191
	As18	0.411342		Sb11	0.891703
	As19	0.406551		Sb12	0.881672
	As20	0.406557		Sb20	0.915651
	As21	0.411324		Sb21	0.887162
	Total for As	3.286614		Total for Sb	7.134608
	Cl22	-0.30776		Cl22	-0.34714
	Cl23	-0.30774		Cl23	-0.32198
	Cl24	-0.33735		Cl24	-0.32852
	Cl168	-0.33736		Cl25	-0.34098
	Total for Cl	-1.29021		Total for Cl	-1.33862
	<i>Total for C</i>	<i>-17.19110</i>		<i>Total for C</i>	<i>-20.51660</i>
	<i>Total for H</i>	<i>18.14539</i>		<i>Total for H</i>	<i>17.98963</i>
	<i>Total for all</i>	<i>1</i>		<i>Total for all</i>	<i>1</i>

Table S11. Selected Second Order Perturbation theory analysis of Fock matrix in NBO basis for **Au₁₃As₈**.

<i>Interactions between Au core atoms and Au-Sb σ^* bonds with $E(2) > 10$ kcal/mol</i>				
Donor NBO (i)	Acceptor NBO (j) [Au/As contribution ratio]	E(2)	E(j)-E(i)	F(i,j)
702 LP (6) Au1	842 BD*(1) Au2-As15 [80/20]	18.45	0.18	0.068
702 LP (6) Au1	954 BD*(1) Au9-As16 [80/20]	18.45	0.18	0.068
702 LP (6) Au1	927 BD*(1) Au7-As20 [81/19]	51.49	0.18	0.111
702 LP (6) Au1	895 BD*(1) Au5-As19 [81/19]	51.49	0.18	0.111
703 LP (7) Au1	884 BD*(1) Au4-As18 [81/19]	11.35	0.17	0.051
703 LP (7) Au1	948 BD*(1) Au8-As21 [81/19]	11.35	0.17	0.051
703 LP (7) Au1	858 BD*(1) Au3-As14 [81/19]	28.98	0.17	0.082
703 LP (7) Au1	999 BD*(1) Au12-As17 [81/19]	28.98	0.17	0.082
703 LP (7) Au1	844 BD*(1) Au2-As15 [80/20]	43.54	0.18	0.104
703 LP (7) Au1	956 BD*(1) Au9-As16 [80/20]	43.54	0.18	0.104
704 LP (8) Au1	896 BD*(1) Au5-As19 [81/19]	20.94	0.17	0.069
704 LP (8) Au1	928 BD*(1) Au7-As20 [81/19]	20.95	0.17	0.069
704 LP (8) Au1	858 BD*(1) Au3-As14 [81/19]	44.06	0.16	0.100
704 LP (8) Au1	999 BD*(1) Au12-As17 [81/19]	44.06	0.16	0.100
704 LP (8) Au1	877 BD*(1) Au4-As18 [81/19]	60.04	0.16	0.115
704 LP (8) Au1	941 BD*(1) Au8-As21 [81/19]	60.05	0.16	0.115

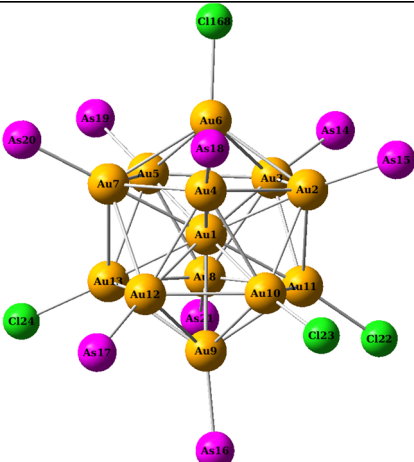
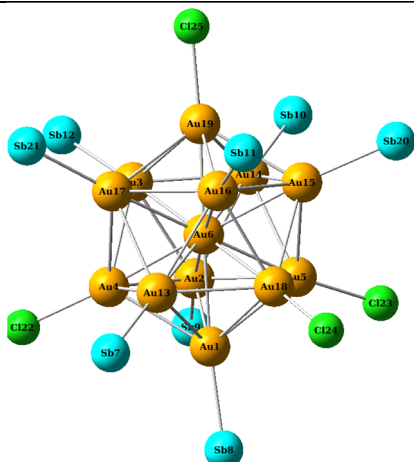
705 LP (9) Au1	884 BD*(1) Au4-As18 [81/19]	12.19	0.03	0.023
705 LP (9) Au1	948 BD*(1) Au8-As21 [81/19]	12.19	0.03	0.023
705 LP (9) Au1	869 BD*(1) Au3-As14 [81/19]	13.83	0.03	0.026
705 LP (9) Au1	999 BD*(1) Au12-As17 [81/19]	13.83	0.03	0.026
705 LP (9) Au1	896 BD*(1) Au5-As19 [81/19]	14.49	0.03	0.028
705 LP (9) Au1	928 BD*(1) Au7-As20 [81/19]	14.49	0.03	0.028
705 LP (9) Au1	852 BD*(1) Au2-As15 [80/20]	16.83	0.04	0.033
705 LP (9) Au1	964 BD*(1) Au9-As16 [80/20]	16.83	0.04	0.033
<i>Interactions between Au core atoms and As-C σ^* bonds with $E(2) > 1.5$ kcal/mol</i>				
Donor NBO (i)	Acceptor NBO (j) [As/C contribution ratio]	E(2)	E(j)-E(i)	F(i,j)
708 LP(3) Au2	843 BD*(1) As15-C26 [63/37]	2.36	0.50	0.031
709 LP(4) Au2	843 BD*(1) As15-C170 [62/38]	1.92	0.51	0.028
709 LP(4) Au2	843 BD*(1) As15-C147 [62/38]	1.69	0.50	0.026
716 LP(3) Au3	859 BD*(1) As14-C63 [62/38]	2.25	0.50	0.030
717 LP(4) Au3	859 BD*(1) As14-C47 [63/37]	2.22	0.50	0.030
724 LP(3) Au4	875 BD*(1) As18-C69 [62/38]	2.32	0.50	0.031
725 LP(4) Au4	875 BD*(1) As18-C226 [62/38]	1.76	0.50	0.027
725 LP(4) Au4	875 BD*(1) As18-C36 [63/37]	1.82	0.49	0.027
732 LP(3) Au5	892 BD*(1) As19-C80 [62/38]	2.22	0.50	0.030
733 LP(4) Au5	892 BD*(1) As19-C192 [63/37]	2.38	0.50	0.031
749 LP(3) Au7	924 BD*(1) As20-C180 [62/38]	2.22	0.50	0.030
750 LP(4) Au7	924 BD*(1) As20-C103 [63/37]	2.38	0.50	0.031
757 LP(3) Au8	939 BD*(1) As21-C246 [62/38]	2.32	0.50	0.031
758 LP(4) Au8	939 BD*(1) As21-C113 [62/38]	1.76	0.50	0.027
758 LP(4) Au8	939 BD*(1) As21-C279 [63/37]	1.82	0.49	0.027
765 LP(3) Au9	955 BD*(1) As16-C125 [63/37]	2.36	0.50	0.031
766 LP(4) Au9	955 BD*(1) As16-C207 [62/38]	1.92	0.51	0.028
766 LP(4) Au9	955 BD*(1) As16-C271 [62/38]	1.69	0.50	0.026
791 LP(3) Au12	794 BD*(1) As17-C160 [62/38]	2.25	0.50	0.030
792 LP(4) Au12	794 BD*(1) As17-C137 [63/37]	2.22	0.50	0.030

Note: The isovalue and density of the NBO orbitals were set to 0.01 and 0.0004, respectively.

<i>Interactions between Au core atoms and Sb-C σ^* bonds with $E(2) > 1.5$ kcal/mol</i>				
Donor NBO (i)	Acceptor NBO (j) [Sb/C contribution ratio]	E(2)	E(j)-E(i)	F(i,j)
587 LP(3) Au1	716 BD*(1) Sb8-C56 [69/31]	1.84	0.48	0.027
588 LP(4) Au1	716 BD*(1) Sb8-C50 [69/31]	1.76	0.47	0.026
595 LP(3) Au2	732 BD*(1) Sb9-C62 [69/31]	2.00	0.48	0.028
596 LP(4) Au2	732 BD*(1) Sb9-C74 [69/31]	1.81	0.47	0.026
603 LP(3) Au3	747 BD*(1) Sb12-C158 [69/31]	1.80	0.48	0.026
604 LP(4) Au3	747 BD*(1) Sb12-C152 [69/31]	1.98	0.47	0.028
638 LP(3) Au13	866 BD*(1) Sb7-C38 [69/31]	2.01	0.47	0.028
639 LP(4) Au13	866 BD*(1) Sb7-C26 [69/31]	1.59	0.47	0.025
646 LP(3) Au14	649 BD*(1) Sb10-C86 [69/31]	1.99	0.47	0.028
647 LP(4) Au14	649 BD*(1) Sb10-C92 [69/31]	1.71	0.47	0.026
663 LP(4) Au16	914 BD*(1) Sb11-C116 [69/31]	2.03	0.47	0.028
654 LP(3) Au15	898 BD*(1) Sb20-C98 [69/31]	1.57	0.48	0.025
655 LP(4) Au15	898 BD*(1) Sb20-C104 [69/31]	1.98	0.48	0.028
670 LP(3) Au17	930 BD*(1) Sb21-C140 [69/31]	1.68	0.48	0.026
671 LP(4) Au17	930 BD*(1) Sb21-C146 [69/31]	1.89	0.47	0.027

Note: The isovalue and density of the NBO orbitals were set to 0.01 and 0.0004, respectively.

Table S13. Selected Wiberg bond indices in the NAO basis for $\text{Au}_{13}\text{As}_8$ and $\text{Au}_{13}\text{Sb}_8$.

$\text{Au}_{13}\text{As}_8$		$\text{Au}_{13}\text{Sb}_8$	
			
Au-As bonds		Au-Sb bonds	
Au12-As17	0.4489	Au3-Sb12	0.5414
Au8-As21	0.4486	Au17-Sb21	0.5408
Au9-As16	0.4823	Au16-Sb11	0.5363
Au3-As14	0.4489	Au15-Sb20	0.5727
Au5-As19	0.4549	Au14-Sb10	0.5363
Au7-As20	0.4549	Au2-Sb9	0.5324
Au4-As18	0.4486	Au13-Sb7	0.5280
Au2-As15	0.4823	Au1-Sb8	0.5658
Average	0.4587	Average	0.5442
Au-Cl bonds		Au-Cl bonds	
Au13-Cl24	0.4073	Au19-Cl25	0.4087
Au11-Cl22	0.4468	Au4-Cl22	0.4015
Au10-Cl23	0.4468	Au18-Cl24	0.4355
Au6-Cl168	0.3696	Au5-Cl23	0.4380
Average	0.4176	Average	0.4209

References

- [1] Rigaku Oxford Diffraction. CrysAlisPro Software system, version 1.171.40.25a, Rigaku Corporation: Oxford, UK, 2018.
- [2] L. Palatinus and G. Chapuis, *J. Appl. Crystallogr.*, 2007, **40**, 786-790.
- [3] O. V. Dolomanov, L. J. Bourhis, R. J. Gildea, J. A. K. Howard and H. Puschmann, *J. Appl. Crystallogr.*, 2009, **42**, 339-341.
- [4] G. M. Sheldrick, *Acta. Crystallogr., Sect. C.*, 2015, **71**, 3-8.
- [5] A. L. Spek, *Acta. Crystallogr. Sect. D.*, 2009, **65**, 148-155.
- [6] Gaussian 16, Rev. B.01, M. J. Frisch, G. W. Trucks, H. B. Schlegel, G. E. Scuseria, M. A. Robb, J. R. Cheeseman, G. Scalmani, V. Barone, G. A. Petersson, H. Nakatsuji, X. Li, M. Caricato, A. V. Marenich, J. Bloino, B. G. Janesko, R. Gomperts, B. Mennucci, H. P. Hratchian, J. V. Ortiz, A. F. Izmaylov, J. L. Sonnenberg, Williams, F. Ding, F. Lipparini, F. Egidi, J. Goings, B. Peng, A. Petrone, T. Henderson, D. Ranasinghe, V. G. Zakrzewski, J. Gao, N. Rega, G. Zheng, W. Liang, M. Hada, M. Ehara, K. Toyota, R. Fukuda, J. Hasegawa, M. Ishida, T. Nakajima, Y. Honda, O. Kitao, H. Nakai, T. Vreven, K. Throssell, J. A. Montgomery Jr., J. E. Peralta, F. Ogliaro, M. J. Bearpark, J. J. Heyd, E. N. Brothers, K. N. Kudin, V. N. Staroverov, T. A. Keith, R. Kobayashi, J. Normand, K. Raghavachari, A. P. Rendell, J. C. Burant, S. S. Iyengar, J. Tomasi, M. Cossi, J. M. Millam, M. Klene, C. Adamo, R. Cammi, J. W. Ochterski, R. L. Martin, K. Morokuma, O. Farkas, J. B. Foresman and D. J. Fox, Wallingford, CT, 2016.
- [7] C. Adamo and V. Barone, *J. Chem. Phys.*, 1998, **108**, 664-675.
- [8] Q. S. Li, B. Xu, Y. M. Xie, R. B. King and H. F. Schaefer, *Dalton Trans.*, 2007, 4312-4322.
- [9] P. J. Hay and W. R. Wadt, *J. Chem. Phys.*, 1985, **82**, 299-310.
- [10] M. J. Frisch, J. A. Pople and J. S. Binkley, *J. Chem. Phys.*, 1984, **80**, 3265-3269.
- [11] Y.-Z. Li, R. Ganguly, K. Y. Hong, Y. Li, M. E. Tessensohn, R. Webster and W. K. Leong, *Chem. Sci.*, 2018 **9**, 8723-8730.
- [12] T. Lu and F. Chen, *J. Comput. Chem.*, 2012, **33**, 580-592.
- [13] M.-C. Brandys, M. C. Jennings and R. J. Puddephatt, *J. Chem. Soc. Dalton*, 2000, 4601-4606.
- [14] Y.-Z. Li and W. K. Leong, *RSC Adv.*, 2019, **9**, 5475-5479.
- [15] N. A. Barnes, K. R. Flower, S. M. Godfrey, P. A. Hurst, R. Z. Khan and R. G. Pritchard, *CrystEngComm.*, 2010, **12**, 4240-4251.

- [16] R. C. B. Copley and D. M. P. Mingos, *J. Chem. Soc. Dalton*, 1996, 491-500.
- [17] Y. Shichibu, K. Suzuki and K. Konishi, *Nanoscal*, 2012, **4**, 4125-4129.
- [18] Z. Lei, J. J. Li, Z. A. Nan, Z. G. Jiang and Q. M. Wang, *Angew. Chem. Int. Ed.*, 2021, **60**, 14415-14419.
- [19] L. C. McKenzie, T. O. Zaikova and J. E. Hutchison, *J. Am. Chem. Soc.*, 2014, **136**, 13426-13435.